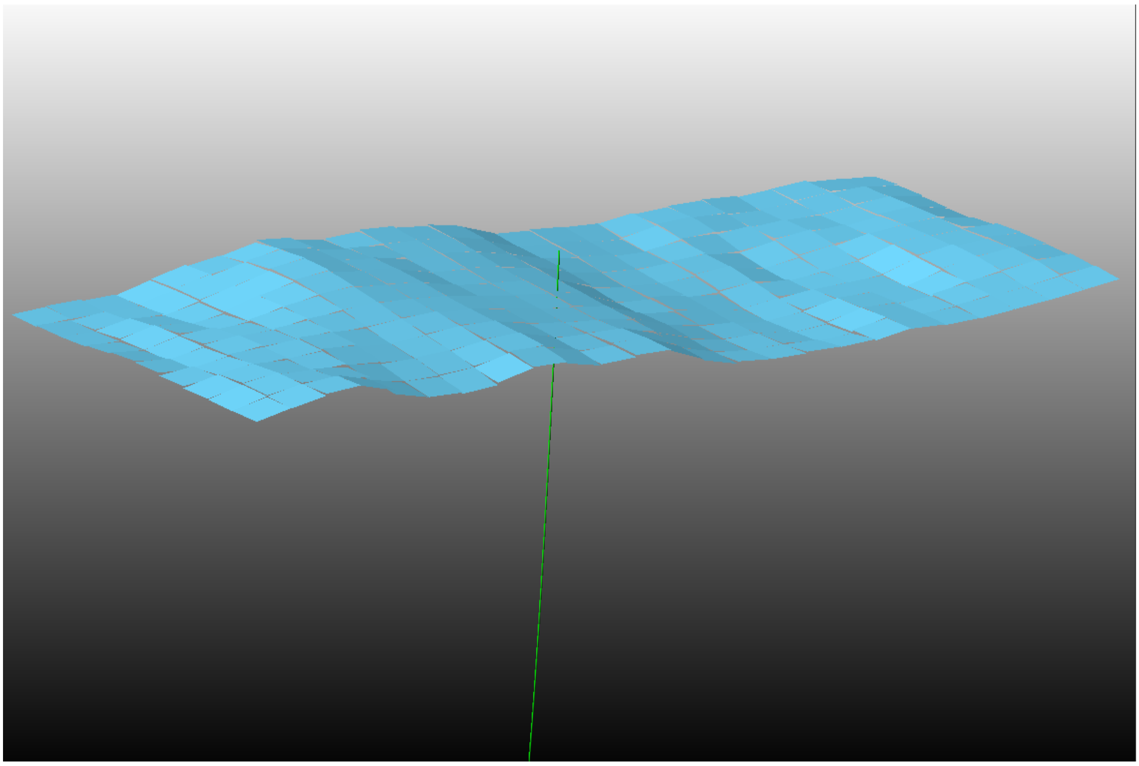

Implementation of sea loads in Adams

Master's thesis in Dynamics

LILLY MA

JONATHAN RYDBERG

Department of Applied Mechanics
Division of Dynamics
CHALMERS UNIVERSITY OF TECHNOLOGY
Gothenburg, Sweden 2014

Master's thesis 2014:02

MASTER'S THESIS IN DYNAMICS

Implementation of sea loads in Adams

LILLY MA
JONATHAN RYDBERG

Department of Applied Mechanics
Division of Dynamics
CHALMERS UNIVERSITY OF TECHNOLOGY

Gothenburg, Sweden 2014

Implementation of sea loads in Adams
LILLY MA
JONATHAN RYDBERG

Master's thesis 2014:02
ISSN 1652-8557
Department of Applied Mechanics
Division of Dynamics
Chalmers University of Technology
SE-412 96 Gothenburg
Sweden
Telephone: +46 (0)31-772 1000

Cover:
An illustration of a riser pipe in irregular waves

Chalmers Reproservice
Gothenburg, Sweden 2014

Implementation of sea loads in Adams
Master's thesis in Dynamics
LILLY MA
JONATHAN RYDBERG
Department of Applied Mechanics
Division of Dynamics
Chalmers University of Technology

Abstract

It is interesting to be able to calculate the dynamics of a simple structure affected by sea loads from both an academic and an industrial perspective. The focus of this master thesis project was to implement sea loads on simple offshore structures made of cylindrical elements in Adams, a software for multibody system simulation. The thesis resulted in a Adams plug-in.

A subroutine has been created based on relevant theories. The subroutine describes the sea loads on a cylindrical element, including buoyancy, wave loads and current loads. A number of macros, that executes Adams/View commands, have also been created. The macros build riser pipes made of cylindrical elements and apply the subroutine to each element. A dialog box has been designed so that the user can control the macros and the subroutine. Finally everything has been packaged as a plug-in.

To verify the functionality of the plug-in, simulation results from Adams have been compared to both analytical solutions and simulation results from other softwares. The results agree well. However, there are still a number of features left to be verified.

Keywords: wave loads, sea loads, current loads

Preface

This is our final project in Applied Mechanics in Mechanical Engineering at Chalmers University of Technology. The work was performed at MSC Software during the period September 2013 to January 2014. This piece of paper is about sea loads, dynamics and Adams. However, it does not reflect the frustration and tiredness we had to endure when things did not go our way. Neither does it reflect the joy and happiness that we felt when things finally did go our way, but why does it matter? No one can give a better answer to this question than the indian guy in the TV show boston tea party: "The bird technology will interview so many different varieties in the full."

Acknowledgements

First and foremost, we would like to express our sincere gratitude to our supervisor Fredrik Sjögren for the support, for his patience, enthusiasm and immense knowledge. Besides our supervisor, we owe particular thanks to our thesis examiner, Per-åke Jansson, for the valuable guidance. Our thanks also goes to MSC Software Gothenburg for their support and encouragement. We would like to acknowledge the support from 4Subsea. Last but not least, we would like to thank our families and friends, for their devotion and support.

Lilly and Jonathan
Gothenburg, Sweden, 2013

Contents

List of Tables

List of Figures

List of Symbols

Symbol	Unit	Description
$\boldsymbol{\alpha}$	rad/s^2	$\frac{\partial \boldsymbol{\omega}}{\partial t} + \boldsymbol{\Omega} \times \boldsymbol{\omega}$, angular acceleration of the local coordinate system xyz
α	-	Intensity of the spectra, default: $\alpha = 0.0081$
β	-	Shape factor, default: 1.25
γ	-	Peak enhancement factor
ϵ	-	Randomized phase displacement
ζ	m	Wave profile
ζ_a	m	Wave amplitude
θ_c	rad	Current propagation direction
λ	m	Wave length
ξ	m	the z coordinate of the sea surface
ρ_{sw}	kg/m^3	density of sea water
σ	-	0.07 if $\omega \leq \omega_p$, $\sigma = 0.09$ if $\omega > \omega_p$
$\boldsymbol{\omega}$	rad/s	Angular velocity of the local coordinate system xyz
ω	rad/s	Wave frequency
$\omega_{\boldsymbol{p}}$	rad/s	Peak wave frequency
A	m^2	Frontal area of the cylinder
a	-	$\exp(-\frac{(\omega-\omega_p)^2}{2\omega_p^2\sigma^2})$
A_{c}	m^2	Cylinders cross sectional area
$\mathbf{a}_{\mathrm{f}}$	m/s^2	Fluid acceleration vector
$\mathbf{a}_{\mathrm{fn}}$	m/s^2	Fluid acceleration normal to the cylinder's symmetry axis
$\mathbf{a}_{\mathrm{P}}$	m/s^2	Acceleration at point P expressed in the global coordinate system
$\mathbf{a}_{\mathrm{P/O'}}$	m/s^2	Acceleration at point O' expressed in the global coordinate system
$\mathbf{a}_{\mathrm{r}}$	m/s	Relative acceleration vector
$\mathbf{a}_{\mathrm{rn}}$	m/s^2	Fluid acceleration normal to the cylinder's symmetry axis relative to the cylinder
$\mathbf{a}_{\mathrm{w}}$	m/s^2	Wave acceleration vector
a_x, a_y, a_z	m/s^2	Wave acceleration components
C_{A}	-	Added mass coefficient
C_{D}	-	Drag coefficient
D	m	Diameter of the cylinder
dL	m	Length of a subelement
$\mathbf{F}$	N	Force vector
$F(\theta, \omega)$	m^{2}s	wave spectrum as a function of frequency and propagation direction
$f(\theta)$	-	function that describes the directions of the irregular wave component
F_{B}	N	Buoyancy force
$\mathbf{F}_{\mathrm{cyl}}$	N	Morison force on a cylindrical element

$\mathbf{F}_{\mathrm{n}}$	N/m	Force with direction normal to the axis of the cylinder
g	m/s^2	Gravity
h	m	Average water depth
k	1/m	Wave number
L_{w}	m	A scalar, the distance along the axis of symmetry from the lower and center point on the cylinder to the intersection point, so called wetted length
$\mathbf{M}$	Nm	The torque vector
N	-	Total number of wave components
$\vec{\mathbf{n}}$	m	Normal vector to instant sea surface
$\mathbf{P}$	m	Unit vector pointing along the axis of symmetry
p_{a}	Pa	Atmospheric pressure at sea surface
$\mathbf{P}_{\mathrm{b}}$	m	Lowest end center point on a cylindrical element
$\mathbf{P}_{\mathrm{p}}$	m	Arbitrary point in the tangent plane
$\mathbf{r}$	m	Displacement vector, from the point which torque is measured to the point where the force is applied
$\mathbf{r}_{\mathrm{cm}\to\mathrm{i}}$	m/s	Displacement vector from the center of mass for each element to the integration point
$\mathbf{r}_{\mathrm{P/O'}}$	m/s	Displacement vector from the point O' to point P expressed in the global coordinate system
(s_x, s_y, s_z)	m	A vector parallel to the symmetry axis
$S(\omega)$	m^{2}s	Wave spectrum function
T	s	Wave period
$\mathbf{U}$	m/s	Current velocity
$\mathbf{U}_{\mathrm{d}}$	m/s	Density driven current
$\mathbf{U}_{\mathrm{m}}$	m/s	Current due to major ocean circulation
$\mathbf{U}_{\mathrm{s}}$	m/s	Current due to Stokes' drift
$\mathbf{U}_{\mathrm{set-up}}$	m/s	Current due to set-up phenomena
$\mathbf{U}_{\mathrm{t}}$	m/s	Tidal current
$\mathbf{U}_{\mathrm{w}}$	m/s	Current due to local winds
V	m^3	Volume of displaced water
$\hat{\mathbf{v}}$	m	Unit vector pointing upwards along the axis of symmetry
$\mathbf{v}_{\mathrm{c}}$	m/s	Current velocity vector
$\mathbf{v}_{\mathrm{cm}}$	m/s	The velocity at the center of mass of the cylindrical element
$\mathbf{v}_{\mathrm{f}}$	m/s	Fluid velocity vector
$\mathbf{v}_{\mathrm{O'}}$	m/s	Velocity at point O' expressed in the global coordinate system
$\mathbf{v}_{\mathrm{P}}$	m/s	Velocity at point P expressed in the global coordinate system
$\mathbf{v}_{\mathrm{r}}$	m/s	Relative velocity vector
$\mathbf{v}_{\mathrm{rn}}$	m/s	Fluid velocity normal to the cylinder's symmetry axis relative to the cylinder
v_{spline}	m/s	User-defined current profile
$\mathbf{v}_{\mathrm{w}}$	m/s	Wave velocity vector
v_x, v_y, v_z	m/s	Wave velocity components

(x_0, y_0, z_0)	m	A point on symmetry axis
(x_t, y_t)	m	x, y coordinates of the cylinder's center of mass
z	m	The depth beneath the sea surface

1 Introduction

1.1 Project background

MSC Software is a worldwide company that develops engineering softwares such as Adams and MSC Nastran for various industries, mainly for the automotive and aerospace industries. To attract new customers in the offshore industry, MSC Software would like to include sea loads into Adams, a software for multibody system simulation.

In general, sea loads including loads due to currents, waves and buoyancy are very complex and require CFD analyses. However, there exist some theories that describe the sea loads on simple offshore structures analytically. MSC Software wants to implement some of these theories into Adams, making it possible to solve some common offshore structure problems using Adams, this will make it easier for the offshore industry to do accurate simulations to complex mechanical systems.

1.2 Purpose

The purpose of this master thesis is to implement sea loads on simple offshore structures.

1.3 Objectives

This master thesis should result in a user-friendly toolkit in Adams so that sea loads can easily be applied on structures made of cylindrical elements. To achieve this the following five objectives need to be accomplished:

- Study and understand different theories regarding modelling of sea loads
- Investigate which methods that are suitable to implement in Adams
- Implement sea loads on a cylindrical element
- Build or complement an offshore structure model using the cylindrical elements
- Package the sea load functionality as a user-friendly Adams/View plug-in

1.4 Limitations

The thesis is limited to modelling and implementation of sea loads on slender cylindrical structures. Nonlinear wave theory will not be implemented. The current is assumed to be time independent and uni-directional. No physical tests will be executed during the project.

1.5 Approach

A literature review was carried out to get an understanding of different theories regarding sea loads on offshore structures. Relevant theories were then used to implement sea loads on a simple cylindrical element. The modelling started out from a simple one degree of freedom model with only a buoyancy load and progressed by continuously adding complexity, such as more degrees of freedom and other types of sea loads. After all relevant types of sea loads had been implemented on a cylinder with six degrees of freedom, a more complex structure was built using the cylindrical elements. The verification of the model was performed by comparing the results to both analytical solutions and the existing simulation results from the softwares USFOS and OrcaFlex, see [6]. Macros and a dialog box were then created to automate the modelling of offshore structures containing cylindrical elements. Finally the codes were packaged and added to Adams as a plug-in.

1.6 Outline of the report

The outline of the report can be divided into the following chapters:

- Theoretical background (Chapter 2): presents relevant theories used in the thesis.
- Model structure (Chapter 3): gives an overview of the model construction process.
- The dialog box (Chapter 4): describes the created dialog box.
- Pipe construction (Chapter 5): describes the automated pipe construction process.
- Calculation of sea loads (Chapter 6): describes how the sea loads are calculated.
- Wave visualization (Chapter 7): describes how the waves are visualized in Adams.
- Plug-in (Chapter 8): describe how the toolkit was packaged as a plug-in.
- Verification (Chapter 9): presents the results from the verification.
- Conclusion and discussion (Chapter 10): discusses the results from the verification chapter.
- Recommendations (Chapter 11): suggests actions to improve the toolkit.

2 Theoretical background

2.1 Three dimensional motion

According to [7] the velocity of a point P in a body can be calculated with help of two reference frames, one local body-fixed reference frame and a global reference frame, with the following equation:

$$\mathbf{v}_P = \mathbf{v}_{O'} + \boldsymbol{\omega} \times \mathbf{r}_{P/O'} \qquad \textbf{[2.1.1]}$$

where:

$\mathbf{v}_P$ = velocity at point P relative to a global reference frame
$\mathbf{v}_{O'}$ = velocity of the body-fixed reference frame
$\boldsymbol{\omega}$ = angular velocity of the body-fixed reference frame xyz
$\mathbf{r}_{P/O'}$ = displacement vector from the point O' to point P expressed in the global coordinate system

The corresponding acceleration vector of point P can be calculated with the following equation:

$$\mathbf{a}_P = \mathbf{a}_{O'} + \boldsymbol{\alpha} \times \mathbf{r}_{P/O'} + \boldsymbol{\omega} \times (\boldsymbol{\omega} \times \mathbf{r}_{P/O'}) \qquad \textbf{[2.1.2]}$$

where:

$\mathbf{a}_{O'}$ = acceleration of the body-fixed reference frame
$\mathbf{a}_P$ = acceleration at point P relative to a global reference frame
$\boldsymbol{\alpha}$ = angular acceleration of the body-fixed reference frame

2.2 Fluid and relative motion

According to [4], it is general practice to add the current velocity vector to the wave velocity vector when calculating the fluid velocity vector:

$$\mathbf{v}_f = \mathbf{v}_w + \mathbf{v}_c \qquad \textbf{[2.2.1]}$$

$\mathbf{v}_f$ = fluid velocity vector
$\mathbf{v}_w$ = wave velocity vector
$\mathbf{v}_c$ = current velocity vector

The fluid acceleration is approximately equal to the wave acceleration since the current acceleration is insignificant according to [4], see the following equation:

$$\mathbf{a}_f = \mathbf{a}_w \qquad \textbf{[2.2.2]}$$

$\mathbf{a}_f$ = fluid acceleration vector
$\mathbf{a}_w$ = wave acceleration vector

The fluid velocity and acceleration relative to a moving cylinder are calculated with equation 2.2.3-2.2.4. Henceforth, $\mathbf{v}_r$ and $\mathbf{a}_r$ are referred to as the relative velocity and the relative acceleration respectively.

$$\mathbf{v}_r = \mathbf{v}_f - \mathbf{v}_{cyl} \qquad [\mathbf{2.2.3}]$$

$$\mathbf{a}_r = \mathbf{a}_f - \mathbf{a}_{cyl} \qquad [\mathbf{2.2.4}]$$

$\mathbf{v}_r$ = relative velocity vector
$\mathbf{a}_r$ = relative acceleration vector

2.3 Morison's equation

Morison's equation is used to describe the forces on a cylinder due to fluid motion. The Morison force is directed normal to the cylinder axis. Equation 2.3.1 is the most general form of Morison's equation, based on [4].

$$\mathbf{F}_n = \frac{\pi}{4}\rho_{sw} D^2(\mathbf{a}_{fn} + C_A \mathbf{a}_{rn}) + \frac{1}{2}\rho_{sw} C_D D \mathbf{v}_{rn}|\mathbf{v}_{rn}| \qquad [\mathbf{2.3.1}]$$

where:

$\mathbf{F}_n$ = Morison's force with direction normal to the axis of the cylinder
D = diameter of the cylinder
C_D = drag coefficient
C_A = added mass coefficient
A = frontal area of the cylinder
$\mathbf{a}_{fn}$ = normal fluid acceleration relative to earth
$\mathbf{a}_{rn}$ = normal fluid acceleration relative to the cylinder
$\mathbf{v}_{rn}$ = normal fluid velocity relative to the cylinder

The Morison's equation includes two contributions, one is from the drag force and the other is from the hydrodynamic inertia force. The first term is sometimes referred to as the inertia force. It can be divided into a Froude-Krylov force and a hydrodynamic mass force. The second term in the equation 2.3.1 is the drag force. The Morison force is a force per unit length and is positive in the wave propagation direction. The determination of the drag coefficient C_D and the added mass coefficient C_A shall be performed empirically and depends on the chosen wave theory and various parameters, such as the Reynolds number, roughness effect and a relative current number. Typical values for C_D and C_A are 1.0-1.4 and 1.0, respectively, based on the linear theory for a circular cylinder, according to [2]. However, Morison's equation can only be applied when the diameter of the cylinder is small relative to the wave length. Otherwise, the Morison's equation has to be replaced by diffraction theory, see [3].

2.4 Equivalent force systems

Consider figure 2.4.1, a force F_P is acting at point P on a rigid body. It is possible to move that force to another point, Q, and still get the same system response by adding a moment M_Q. If the response is the same for two systems with different set-ups of forces

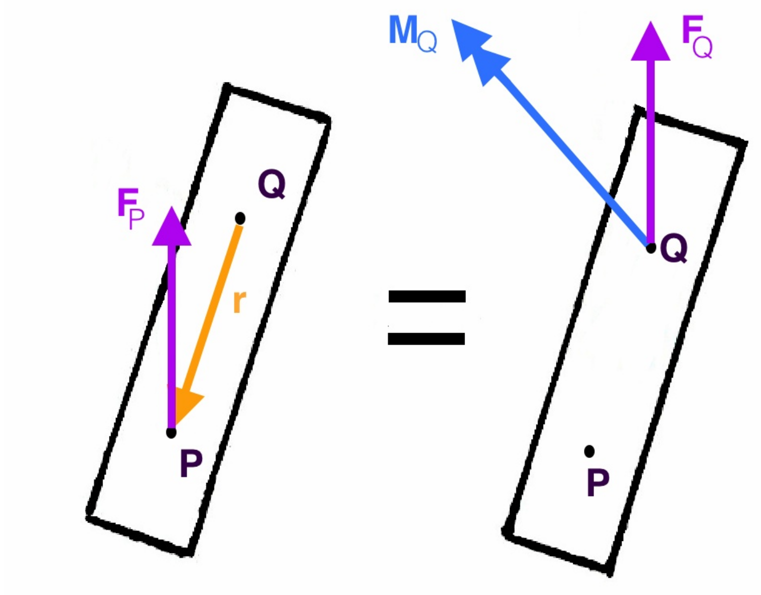

Figure 2.4.1: *Example of three dimensional equivalent force systems*

and moments they are referred to as equivalent force systems. For the systems shown in figure 2.4.1 the force and moment in point Q are described by equations 2.4.1-2.4.2.

$$\mathbf{F}_Q = \mathbf{F}_P \qquad [\mathbf{2.4.1}]$$

$$\mathbf{M}_Q = \mathbf{r} \times \mathbf{F}_P \qquad [\mathbf{2.4.2}]$$

where:

$\mathbf{M}_Q$ = the torque vector
$\mathbf{r}$ = displacement vector QP, see figure 2.4.1
$\mathbf{F}_P$ = force vector

2.5 Archimedes' principle

If a body is situated in water it will be subjected to a buoyancy force. The buoyancy force arises due to a static pressure field that varies linearly with depth, see equation 2.5.1.

$$p = p_a + \rho_{sw} g z \qquad [\mathbf{2.5.1}]$$

where:

p_a = atmospheric pressure at sea surface
ρ_{sw} = density of sea water
g = acceleration of gravity
z = the depth beneath the sea surface

Generally a force due to a varying pressure field is calculated by integrating the pressure over the body surface. In this particular case the pressure field is linear. It could then be shown that the buoyancy force is directed upwards and is governed by equation 2.5.2.

This relationship was discovered by the Greek mathematician Archimedes and is therefore referred to as Archimedes' principle.

$$F_B = \rho_{sw} g V \qquad \textbf{[2.5.2]}$$

where:

F_B = buoyancy force
V = volume of displaced water

2.6 Ocean currents

Currents in the ocean are the result of many independent phenomena. In [1] the current velocity is described by equation 2.6.1.

$$\mathbf{U} = \mathbf{U}_t + \mathbf{U}_w + \mathbf{U}_s + \mathbf{U}_m + \mathbf{U}_{set-up} + \mathbf{U}_d \qquad \textbf{[2.6.1]}$$

where:

$\mathbf{U}$ = current velocity
$\mathbf{U}_t$ = tidal current
$\mathbf{U}_w$ = current due to local winds
$\mathbf{U}_s$ = current due to Stokes' drift
$\mathbf{U}_m$ = current due to major ocean circulation
$\mathbf{U}_{set-up}$ = current due to set-up phenomena
$\mathbf{U}_d$ = density driven current

There exists empirical equations that describe the behaviour of some of the components. However, in a general case these equations give an insufficient prediction of currents. Therefore it is common to simply measure the current profile.

Since the velocity field in a current varies slowly in time relative to the velocity field in a wave the current can be assumed to be stationary, according to [4].

2.7 Ocean waves

In theory, there are three common types of waves, regular waves, irregular waves and nonlinear waves. These will be discussed in this section along with other relevant wave theory.

2.7.1 Underlying theory

To establish the velocity and acceleration fields in a wave it is assumed that the fluid is incompressible and inviscid. The wave should satisfy the continuity equation and some boundary conditions at the surface and at the seabed. The boundary conditions are nonlinear and states that:

- the pressure at the surface is constant (dynamic boundary condition)
- the surface is impermeable (kinematic boundary condition)

- the seabed is impermeable (kinematic boundary condition)

If the the nonlinear boundary conditions are linearized the wave dynamics could be described with relatively simple expressions. These types of waves are referred to as linear waves, which include both regular waves and irregular waves. For a more detailed description of the theory, see [4].

2.7.2 Regular waves

In a regular wave the velocity, the acceleration, the wave profile, the wave frequency, the wave number and wavelength are given by equations 2.7.1-2.7.8.

$$v_x = \omega\zeta_a \frac{\cosh(k(z+h))}{\sinh(kh)} \sin(\omega t - kx\cos(\theta) - ky\sin(\theta)) \quad \textbf{[2.7.1]}$$

$$v_z = \omega\zeta_a \frac{\sinh(k(z+h))}{\sinh(kh)} \cos(\omega t - kx\cos(\theta) - ky\sin(\theta)) \quad \textbf{[2.7.2]}$$

$$a_x = \omega^2\zeta_a \frac{\cosh(k(z+h))}{\sinh(kh)} \cos(\omega t - kx\cos(\theta) - ky\sin(\theta)) \quad \textbf{[2.7.3]}$$

$$a_z = -\omega^2\zeta_a \frac{\sinh(k(z+h))}{\sinh(kh)} \sin(\omega t - kx\cos(\theta) - ky\sin(\theta)) \quad \textbf{[2.7.4]}$$

$$\zeta = \zeta_a \sin(\omega t - kx\cos(\theta) - ky\sin(\theta)) \quad \textbf{[2.7.5]}$$

$$\omega = \frac{2\pi}{T} \quad \textbf{[2.7.6]}$$

$$k = \frac{2\pi}{\lambda} \quad \textbf{[2.7.7]}$$

$$\lambda = \frac{g}{2\pi} T^2 \tanh(\frac{2\pi}{\lambda} h) \quad \textbf{[2.7.8]}$$

where:

v_x, v_y, v_z	= wave velocity components
a_x, a_y, a_z	= wave acceleration components
ω	= wave frequency
T	= wave period
ζ_a	= wave amplitude
k	= wave number
λ	= wave length
h	= average water depth
ζ	= wave profile
z	= wave z-position with respect to the mean sea surface
θ	= wave angle

To describe a regular wave the wave amplitude and either the wave period or the wavelength has to be specified. It is most common that the wave period is specified. Note that equation

2.7.8 is an implicit function, as a consequence λ has to be solved iteratively for a specified wave period.

For regular waves it is common to distinguish between finite and infinite water depth. If $\frac{h}{\lambda} > 0.5$ the water is considered infinitely deep and a number of simplifications can be made to equations 2.7.1-2.7.8. The biggest gain of assuming infinite water depth is that $tanh(\frac{2\pi}{\lambda}h) \rightarrow 1$, turning equation 2.7.8 into an explicit function and λ could be calculated directly.

As discussed in section 2.7.1 the regular waves are a result of linearized boundary conditions. As a consequence the regular waves only give good results when the wave steepness is low. That is the wave height, i.e. H, is small relative to the wave length, λ. The meaning of a low wave steepness in this context may vary depending on the purpose of the analysis.

2.7.3 Extension methods

Equations 2.7.1-2.7.8 are only valid from the seabed to the mean sea surface. This is a bit problematic since the field variables, such as the velocity and acceleration, is then unknown between the wave crest and the mean sea surface.

The simplest way to deal with this issue is to assign all field variables above the mean sea surface their corresponding mean sea surface value. This method is known as constant extension, see figure 2.7.1.

Another way to deal with the issue is to do an extrapolation of higher order. For example, the tangent at the mean sea surface could be used to make a linear extrapolation. This type of extrapolation method is known to exaggerate the magnitude of the field variables.

It is also possible to stretch out the profile of the field variable. This is done by evaluating eq 2.7.1-2.7.4 at a displaced z coordinate, z', see equation 2.7.9. Wheeler stretching and constant extension are shown in figure 2.7.1.

$$z' = z\frac{h}{h+\xi} + h(\frac{h}{h+\xi} - 1) \qquad \textbf{[2.7.9]}$$

where:

ξ = the z-coordinate of the sea surface

All extension methods can also be used on a current profile. It is therefore sufficient to define the current field from the mean sea surface to the seabed. It should be noted that wheeler stretching is used differently for currents. The current profile is stretched under the wave crest, but unlike the wave field variables it is also compressed under the wave thrust.

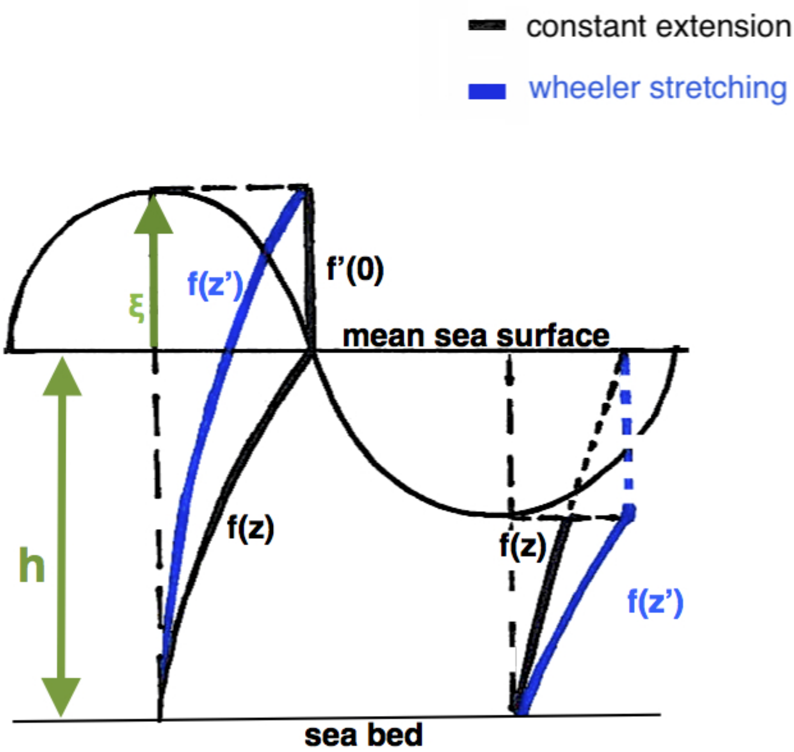

Figure 2.7.1: *An illustration of wheeler stretching and constant extension*

2.7.4 Irregular waves

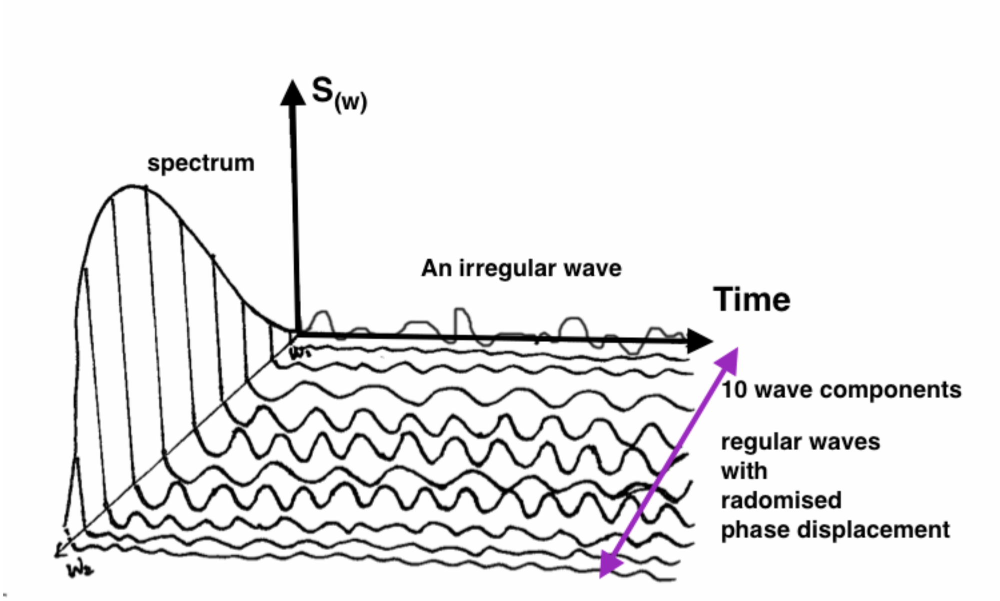

Figure 2.7.2: *The irregular wave components generated by a wave spectrum*

The perk of utilizing regular waves are that these are linear in the sense that two or more different regular waves could be summed and thus make a new wave, a so called irregular wave. The velocity field, acceleration field and wave profile for such a wave are described by equations 2.7.10-2.7.14.

$$v_x = \sum_{j=1}^{N} \omega_j \zeta_j \frac{\cosh(k_j(z+h))}{\sinh(k_j h)} \sin(\omega_j t - k_j x cos(\theta) - k_j y \sin(\theta) + \epsilon_j) \qquad \textbf{[2.7.10]}$$

$$v_z = \sum_{j=1}^{N} \omega_j \zeta_j \frac{\sinh(k_j(z+h))}{\sinh(k_j h)} \cos(\omega_j t - k_j x \cos(\theta) - k_j y \sin(\theta) + \epsilon_j) \qquad \textbf{[2.7.11]}$$

$$a_x = \sum_{j=1}^{N} \omega_j^2 \zeta_j \frac{\cosh(k_j(z+h))}{\sinh(k_j h)} \cos(\omega_j t - k_j x \cos(\theta) - k_j y \sin(\theta) + \epsilon_j) \qquad \textbf{[2.7.12]}$$

$$a_z = -\sum_{j=1}^{N} \omega_j^2 \zeta_j \frac{\sinh(k_j(z+h))}{\sinh(k_j h)} \sin(\omega_j t - k_j x \cos(\theta) - k_j y \sin(\theta) + \epsilon_j) \qquad \textbf{[2.7.13]}$$

$$\zeta = \sum_{j=1}^{N} \zeta_j \sin(\omega_j t - k_j x \cos(\theta) - k_j y \sin(\theta) + \epsilon_j) \qquad \textbf{[2.7.14]}$$

where:

ϵ_j = randomized phase displacement
j = the j:th wave component
N = total number of wave components

ζ, ζ_j, ω_j, k_j are explained in section 2.7.2. The field variables for an irregular wave are obtained simply by summing different set-ups of equation 2.7.1-2.7.5 and adding a randomized phase displacement.

To create a realistic sea state a wave spectrum should be used. A wave spectrum is created based on measurements of waves in the ocean. It defines the constellation of regular waves that occur in an irregular wave. A wave spectrum expresses how the energy is distributed over the wave frequencies, $S(\omega)$. For a certain wave frequency, ω_j, the corresponding wave number, k_j, is obtained in the same way as for a regular wave. The wave amplitude however is obtained by equation 2.7.15.

$$\zeta_j = \sqrt{2 \int_{\omega_{jL}}^{\omega_{jU}} S(\omega)\, d\omega} \qquad \textbf{[2.7.15]}$$

where:

ω_{jU} = upper boundary of the j:th bar in the wave spectrum
ω_{jL} = lower boundary of the j:th bar in the wave spectrum

2.7.5 The Pierson-Moskowitz spectrum

To create a wave spectrum Pierson and Moskowitz assumed that: if the wind blows with constant speed over a sufficiently large area, the resulting waves will reach an equilibrium state, referred to as a fully developed sea. Pierson and Moskowitz investigated fully developed seas in the North Atlantic and concluded that it could be described with equation 2.7.16, see [9]. There exists empirical equations that relates ω_p to the wind speed, this is

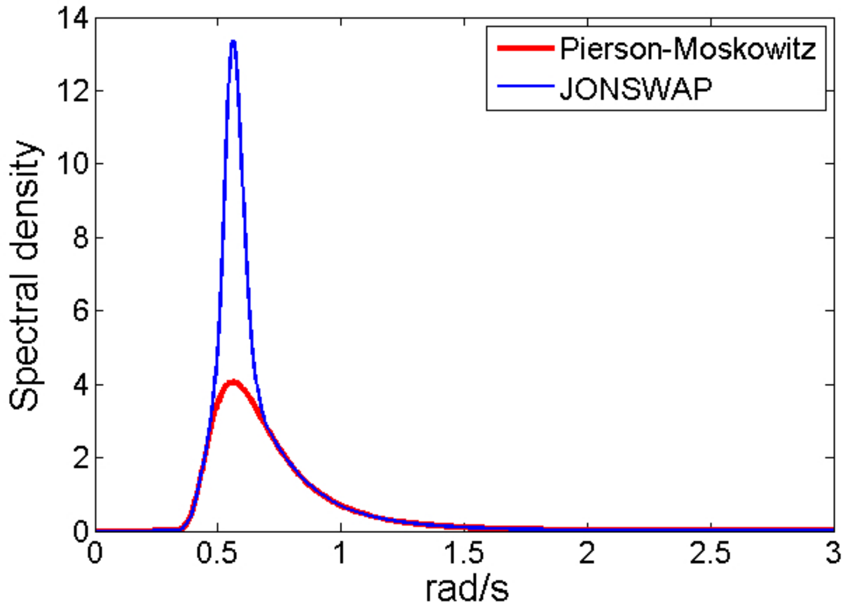

Figure 2.7.3: *The Pierson-Moskowitz spectrum and the JONSWAP spectrum*

very useful since it is easier to specify the wind speed than ω_p. The Pierson-Moskowitz spectrum is shown in figure 2.7.3.

$$S(\omega) = \frac{\alpha g^2}{\omega^5} \exp\left(-\beta \left(\frac{\omega_p}{\omega}\right)^4\right) \qquad \textbf{[2.7.16]}$$

where:

α = intensity of the spectrum, default: $\alpha = 0.0081$
β = shape factor, default: 1.25
ω_p = peak wave frequency

2.7.6 The JONSWAP spectrum

During the Joint North Sea Wave Observation Project, JONSWAP, it was found that a fully developed sea in the Pierson-Moskowitz sense does not exist. The waves with frequencies around the wave peak continue to grow with the distance travelled. To cope with this phenomenon the Pierson-Moskowitz spectrum was modified to equation 2.7.17, see [8]. A JONSWAP spectrum is shown in figure 2.7.3.

$$S(\omega) = \frac{\alpha g^2}{\omega^5} \exp\left(-\beta \left(\frac{\omega_p}{\omega}\right)^4\right) \gamma^a \qquad \textbf{[2.7.17]}$$

where:

γ = peak enhancement factor, default: $\gamma = 3.3$
$a = \exp(-\frac{(\omega-\omega_p)^2}{2\omega_p^2\sigma^2})$
$\sigma = 0.07$ if $\omega \leq \omega_p$, $\sigma = 0.09$ if $\omega > \omega_p$

2.7.7 Directional spectrum

A irregular wave is propagating in a single direction. If only one wave spectrum is used the resulting irregular wave will also propagate in one direction. In a real ocean waves propagate in different directions. To introduce that behaviour in a realistic way a directional spectrum, $f(\theta)$, could be multiplied with the wave spectrum. Thus creating a new 2-dimensional spectrum that takes the propagation direction into account, see eq 2.7.18. A directional spectrum often used to describe short crested waves is given by equation 2.7.19.

$$F(\omega, \theta) = S(\omega) f(\theta) \qquad \textbf{[2.7.18]}$$

$$f(\theta) = \begin{cases} \frac{2}{\pi}\cos^2(\theta - \theta_w) & \text{if } -\frac{\pi}{2} + \theta_w \leq \theta \leq \frac{\pi}{2} + \theta_w \\ 0 & \text{elsewhere} \end{cases} \qquad \textbf{[2.7.19]}$$

To include the directional spectrum in an irregular wave equation, equations 2.7.10-2.7.15 are modified to equations 2.7.20- 2.7.25

$$v_x = \sum_{j=1}^{N}\sum_{k=1}^{M} \omega_j \zeta_{jk} \frac{\cosh(k_j(z+h))}{\sinh(k_j h)} \sin(\omega_j t - k_j x\cos(\theta_k) - k_j y \sin(\theta_k) + \epsilon_{jk}) \qquad \textbf{[2.7.20]}$$

$$v_z = \sum_{j=1}^{N}\sum_{k=1}^{M} \omega_j \zeta_{jk} \frac{\sinh(k_j(z+h))}{\sinh(k_j h)} \cos(\omega_j t - k_j x\cos(\theta_k) - k_j y \sin(\theta_k) + \epsilon_{jk}) \qquad \textbf{[2.7.21]}$$

$$a_x = \sum_{j=1}^{N}\sum_{k=1}^{M} {\omega_j}^2 \zeta_{jk} \frac{\cosh(k_j(z+h))}{\sinh(k_j h)} \cos(\omega_j t - k_j x\cos(\theta_k) - k_j y \sin(\theta_k) + \epsilon_{jk}) \qquad \textbf{[2.7.22]}$$

$$a_z = -\sum_{j=1}^{N}\sum_{k=1}^{M} {\omega_j}^2 \zeta_{jk} \frac{\sinh(k_j(z+h))}{\sinh(k_j h)} \sin(\omega_j t - k_j x\cos(\theta_k) - k_j y \sin(\theta_k) + \epsilon_{jk}) \qquad \textbf{[2.7.23]}$$

$$\zeta = \sum_{j=1}^{N}\sum_{k=1}^{M} \zeta_{jk} \sin(\omega_j t - k_j x\cos(\theta_k) - k_j y \sin(\theta_k) + \epsilon_{jk}) \qquad \textbf{[2.7.24]}$$

$$\zeta_{jk} = \sqrt{2\int_{\omega_{jL}}^{\omega_{jU}} \int_{\theta_{kL}}^{\theta_{kU}} S(\omega, \theta)\, d\omega d\theta} \qquad \textbf{[2.7.25]}$$

2.7.8 Discetization of wave spectrum

The wave spectrum must be discretized in order to create an irregular wave. Two common discretization methods will be discussed in detail in the following subsections.

Equal frequency spacing

Equal frequency spacing is the simplest discretization method. The wave spectrum is simply divided into bars of equal width. Each bar defines a wave component in the irregular wave. The frequency value in the center of the bar defines the wave frequency and the area of the bar is used in equation 2.7.25 to define the wave amplitude. The equal frequency spacing is illustrated in figure 2.7.4.

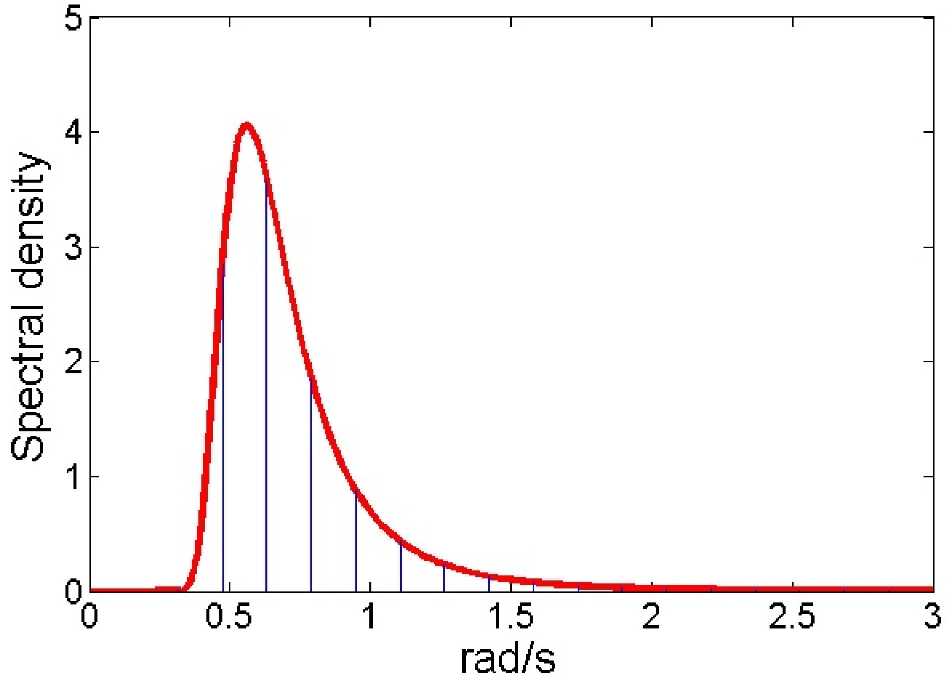

Figure 2.7.4: *The equal frequency spacing method*

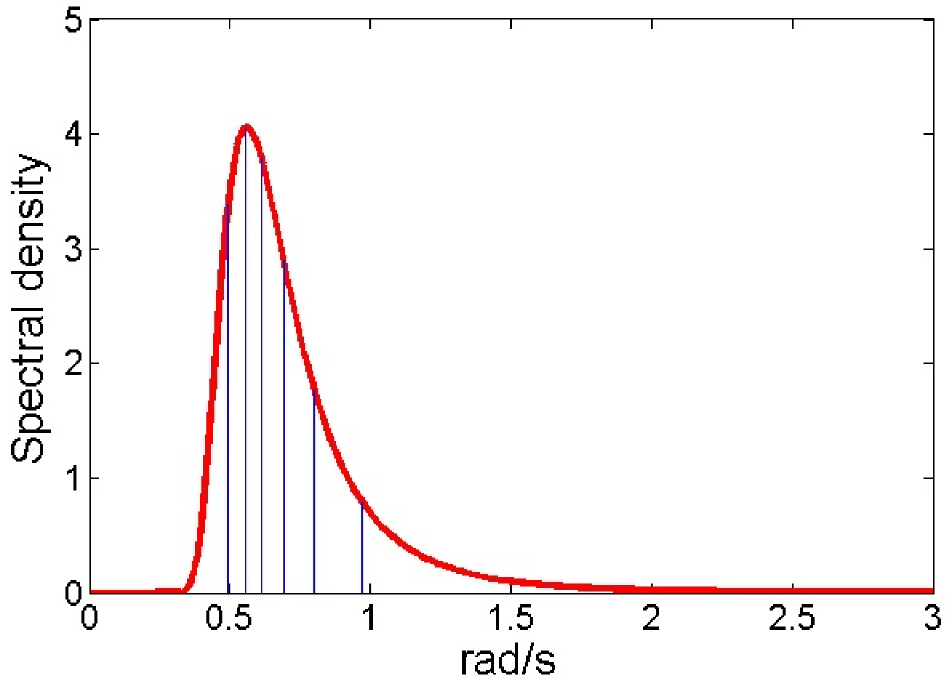

Figure 2.7.5: *The equal energy approach*

Equal energy approach

In the equal energy approach the wave spectrum is divided into bars of equal area. Like the equal frequency spacing approach each bar defines a wave component in the irregular wave. The wave frequency of each wave component is chosen so that the area of the bar below the chosen frequency is equal to the area above the chosen frequency. The area of the bar is used in equation 2.7.25 to define the wave amplitude. It should be noted that the amplitude is the same for all wave components since the areas of the bars are the same. The equal energy approach discretization is illustrated in figure 2.7.5. As a consequence the maximum amplitude of the irregular wave is usually larger when the equal energy approach is used compared to when equal frequency spacing is used. The irregular waves generated with this method are usually less periodical than those generated with equal frequency spacing.

2.7.9 Nonlinear waves

If the nonlinearities in the boundary conditions described in section 2.7.1 are preserved to some extent, the resulting waves are called nonlinear waves. A popular nonlinear wave theory are the Stokes' theory. By making some assumptions Stokes concluded that the field variables in a wave could be calculated with a Fourier expansion. The more terms that are included in the Fourier expansion the better the solution becomes, but on the other hand the solution becomes more complex. The type of Stokes wave used is usually named after the number of terms included in the Fourier expansion. For example if two terms are used the resulting wave are referred to as a 2nd order Stokes wave.

Nonlinear wave theory gives a more accurate description of a wave than linear wave theory. Typically nonlinear waves gets sharper and higher crests and a more shallow thrust than linear waves. The main advantage of using linear waves are that they could be used to create irregular waves, see section 2.7.4, this is not possible with nonlinear waves. Another advantage with linear waves are that ocean currents can be included by just adding the current velocity field to the wave velocity field. In nonlinear wave theory the ocean current will modify the wave shape, so the underlying differential equations need to be reformulated and resolved for every current field.

3 Model structure

The outcome of this master thesis project is a pipe construction toolkit. The toolkit is designed to build straight pipes and is therefore suitable to use when modeling riser pipes. A riser pipe is a long straight vertical pipe that is used to pump oil in the offshore industry. In this chapter the basic structure of the pipe model and the pipe construction toolkit will be discussed.

3.1 Basic set-ups

The pipe is constructed out of cylindrical elements. Furthermore, each cylindrical element is divided into a number of subelements. An illustration of a pipe structure is shown in figure 3.1.1. The cylindrical elements are rigid bodies connected with beams. Increasing the number of cylindrical elements will improve the structural dynamics of the pipe. The subelements are a theoretical division of the cylindrical elements used for numerical integration. The center point of a subelement is referred to as an integration point. When integrating, the relevant field variables are evaluated at the integration points and assumed to be constant over each subelement.

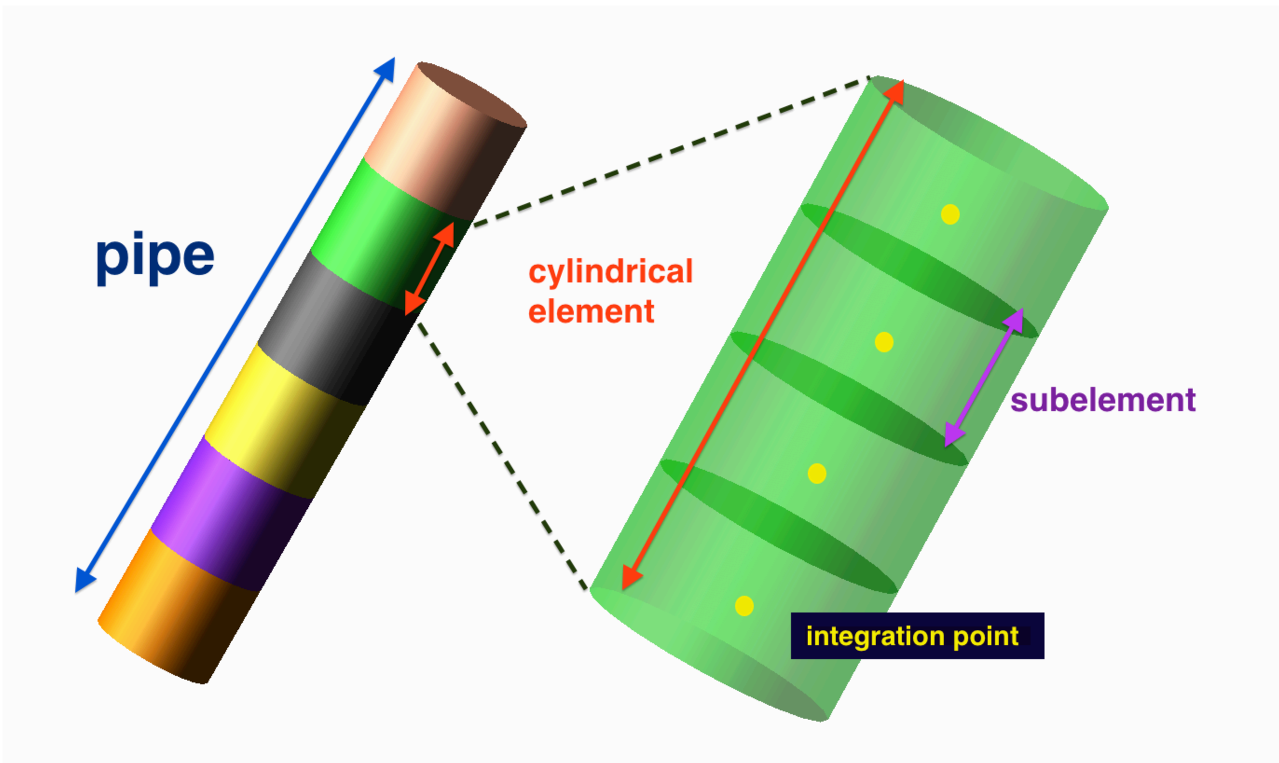

Figure 3.1.1: *A pipe created by the pipe construction toolkit*

In Adams, the coordinate systems are referred to as markers, the origin of a marker also specifies an interactable point. For example, if the user wants to add a spring into the model, the ends of the spring must be attached to the origins of two markers. When creating a new model, a global fixed coordinate system is set by default, it defines the global origin of the model and is used as a basic reference. A 'ref_sea' marker is set at the origin, (0,0,0), and has the same orientation as the global coordinate system. The x, y plane of 'ref_sea' defines the mean sea surface and the z axis is pointing towards the sky. Hence, gravity needs to be oriented in the negative z direction for the model to work properly. 'ref_sea' is also a important reference frame, henceforth it will be referred to the global coordinate system. Every cylindrical element has a 'gforce' marker placed in the center of the cylinder. The 'gforce' marker is another important reference frame. All forces acting on a each cylinder are expressed in this system.

3.2 Toolkit structure

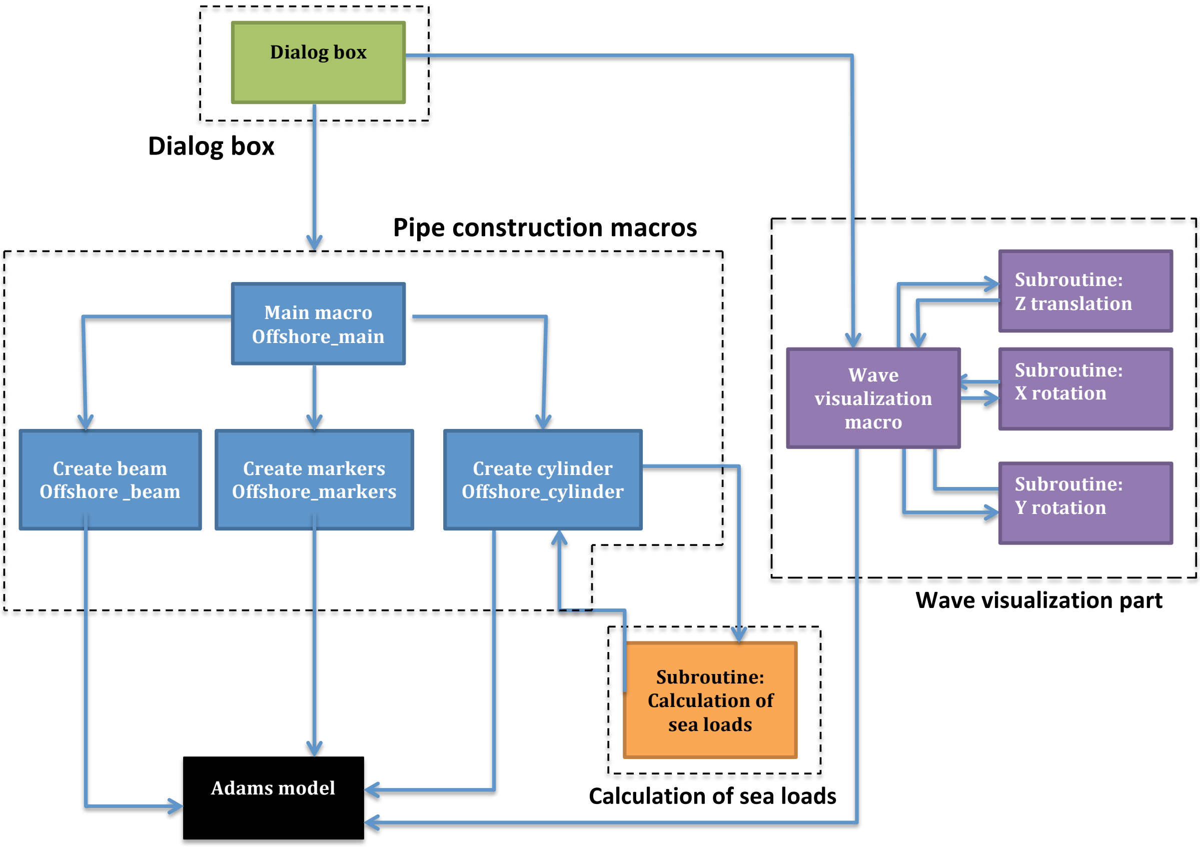

Figure 3.2.1: *An overview of the pipe construction toolkit*

The pipe construction toolkit comprises four main parts, the dialog box, the pipe construction macros, a subroutine that calculates the sea loads, and a wave visualization part. Figure 3.2.1 shows an overview of the structure of the the pipe construction toolkit. The dialog box, discussed in chapter 4, is the toolkit's graphical user interface. It retrieves all user inputs and sends them to the pipe construction macros, discussed in chapter 5, and the wave visualization part, discussed in chapter 7. The pipe construction macros is a generic name for a set of macros that will create a pipe in accordance with the user preferences. These macros will also process the user input and forward it to a subroutine, discussed in chapter 6, that calculates the sea loads acting on the pipe. During a simulation the subroutine will be called in every time step, calculate the sea load and send back that information to the cylindrical elements. As mentioned above there is also a visualization part included in the toolkit. The wave visualization part consists of a macro that creates plates that are used to visualize the sea surface. It also consists of three subroutines that define the motion of the plates.

4 The dialog box

To be able to define the parameters required to utilize the model construction and the wave visualization macros, an Adams dialog box was created. Throughout this chapter different terms related to the interface of dialog box are frequently used, these are shown shown in figure 4.0.1.

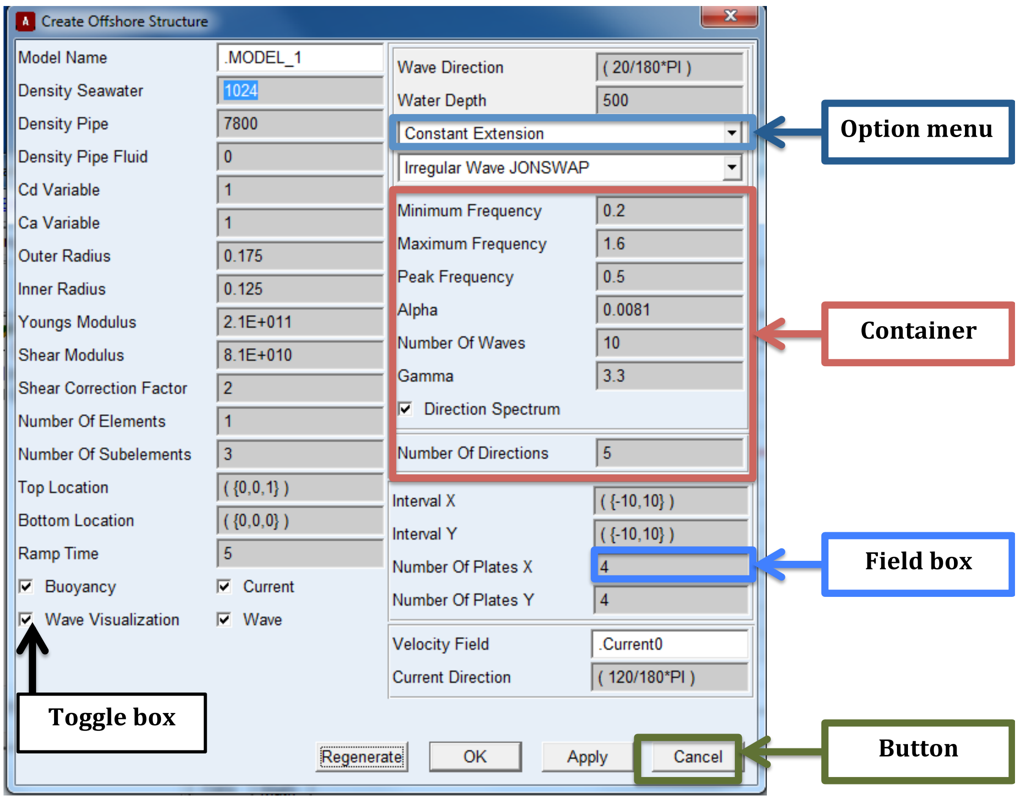

Figure 4.0.1: *The name of the dialog box's components*

4.1 Macro structure

When the user interacts with the dialog box there are a number of underlying macros that executes the user's actions. For example, if the user checks the 'Current' toggle box, the checked box is transformed into a input parameter to a macro connected to that box. The macro is executed every time the button is clicked. The macro structure behind the dialog box is shown graphically in figure 4.1.1. In this particular case the macro will show the current container and activate the current by modifying a parameter.

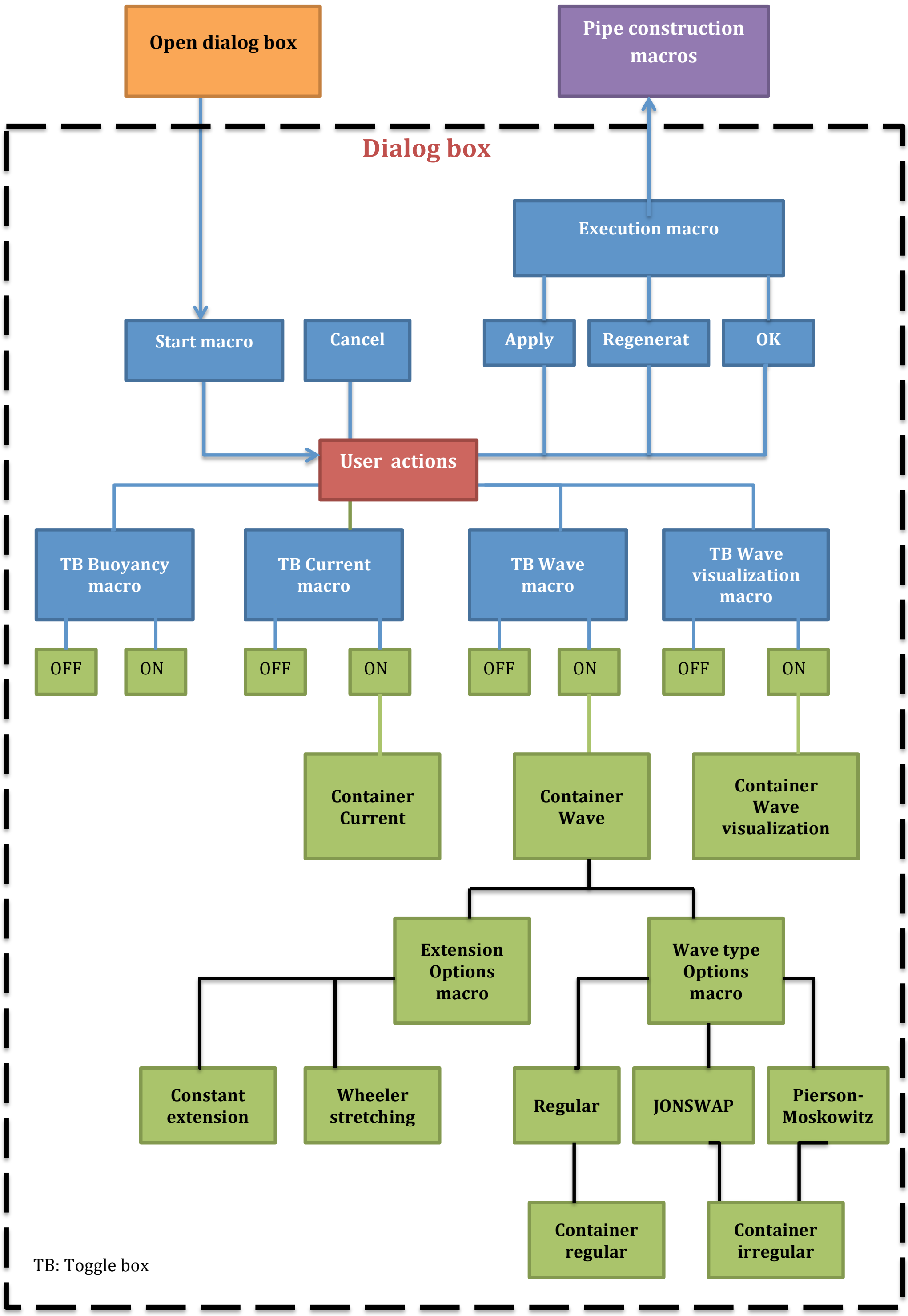

Figure 4.1.1: *A detailed picture of the structure of the dialog box*

When the user opens up the dialog box the 'start macro' is executed. The 'start macro' sets the default appearance of the dialog box, see figure 4.1.2, sets all internal macro parameters so that these correspond to the default appearance, fills all the field boxes with default values and creates the current velocity spline, 'current0'. A spline in this context is a smooth curve fitted to table data containing the current velocity and the corresponding z-coordinates. If the 'Buoyancy' toggle box is pressed a macro will modify a parameter that controls the buoyancy force. The macros connected to the 'Current', 'Wave', 'Wave

Visualization' and the 'Direction Spectrum' toggle boxes and the two option menus in the wave container works in a similar way. In addition these macros show or hide the containers discussed in section 4.2.

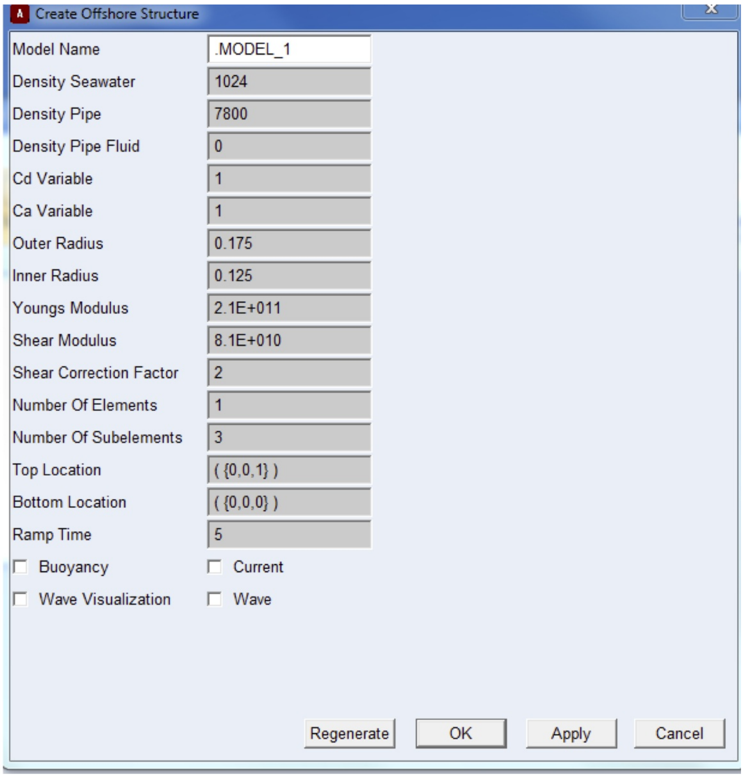

Figure 4.1.2: *The start up appearance of the dialog box*

At any time the user can choose to press on the 'Regenerate', 'OK', 'Apply' or 'Cancel' button. If the 'Apply' button is pressed the 'execution macro' will run. The 'execution macro' calls the 'pipe construction macros' discussed in section 5 and forwards the user specified input parameters. If pressed, the 'OK' and 'Regenerate' button will also call the 'execution macro'. In addition 'OK' will shut down the dialog box while 'Regenerate' will delete everything previously created by the 'pipe construction macros'. Pressing the 'Cancel' button will only shut down the dialog box.

4.2 Appearance

Figure 4.0.1 shows the dialog box when all containers are shown, and table 4.2.1 gives a short description of all the input parameters. To the left some field boxes are shown, these are the basic input parameters and must be filled out to run the program. At the left bottom of the dialog box four toggle boxes can be seen, these are unchecked by default. If the 'Buoyancy' toggle box is checked the buoyancy force will be activated. If the 'Current' toggle box is checked, the current will be activated and a container where current data need to be filled in appears. If the 'Wave Visualization' toggle box is checked, the wave visualization feature will be activated and a container where relevant data need to be filled in will appear. If the 'Wave' toggle box is checked a container will appear. There are two option menus in that container. In the first one the extension method must be selected, two options are available: 'Wheeler Stretching' and 'Constant Extension'. In the second option menu the type of wave must be selected. Three wave types are available: 'Regular Wave', 'Irregular Wave Pierson Moskowitz ' and 'Irregular Wave JONSWAP'. If 'Regular Wave' is chosen, another container appears where regular wave data needs to be filled in, see figure 4.2.1. If 'Irregular Wave Pierson Moskowitz ' or 'Irregular Wave JONSWAP' is chosen, a container appears where irregular wave data needs to be filled in, see figure 4.2.2. The difference between the two latter options is that the parameter 'gamma' cannot be changed when 'Irregular Wave Pierson Moskowitz ' is chosen. In the irregular wave container there is a Direction Spectrum toggle box. If this is checked the direction spectrum will be activated and yet another container appears. The number of directions for the irregular waves must be defined.

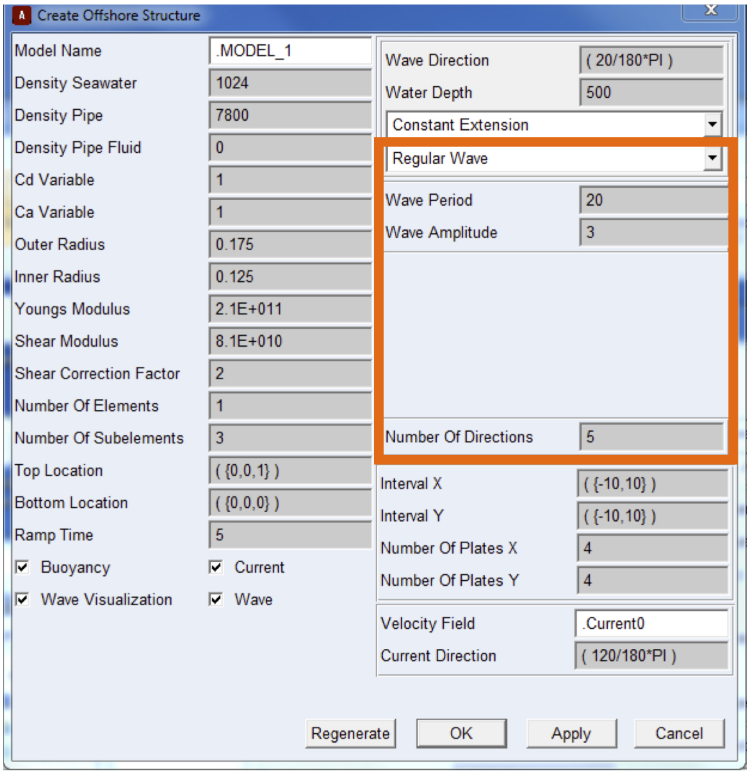

Figure 4.2.1: *When regular waves are chosen*

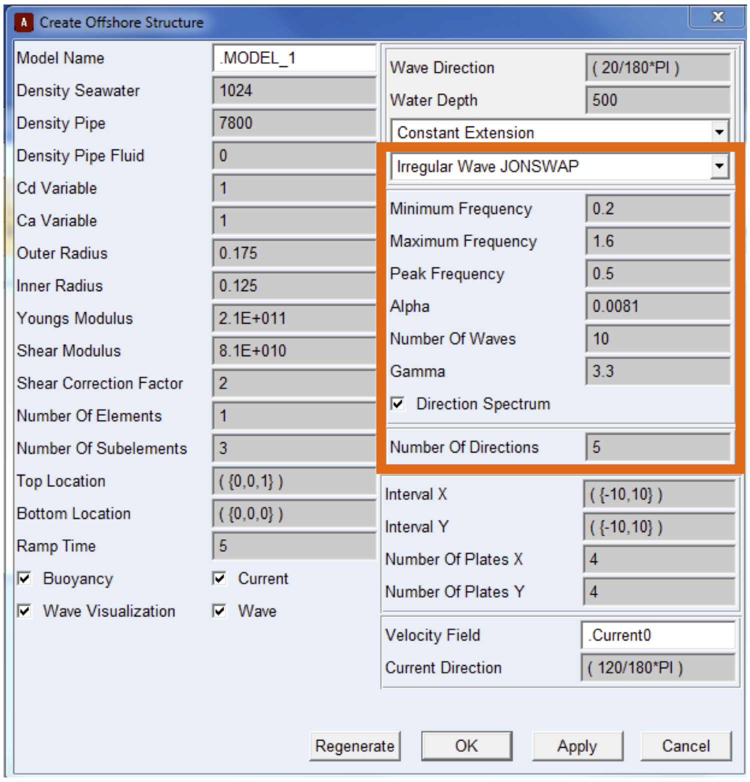

Figure 4.2.2: *When irregular waves are chosen*

Table 4.2.1: User input parameters

Input parameter	**Default value**	**Design variable**	**Description**
Model Name	-	No	The name of the model
Density Seawater, ρ_{w}	1024 [kg/m^3]	Yes	The density of the seawater
Density Pipe, ρ_{p}	800 [kg/m^3]	Yes	The density of the pipe
Density Pipe Fluid, ρ_{f}	1024 [kg/m^3]	Yes	The density of pipes internal fluid
C_{D}	1	Yes	The drag coefficient
C_{A}	1	Yes	The added-mass coefficient
Outer Radius, r_{o}	0.1 [m]	Yes	The outer radius of the pipe
Inner Radius, r_{i}	0.05 [m]	Yes	The inner radius of the pipe
Young's Modulus, E	210 [GPa]	Yes	The Young's modulus of the pipe
Shear Modulus, G	81 [GPa]	Yes	The shear modulus of the pipe
Shear Correction Factor, κ	2	Yes	Correction factor from the Timoshenko beam theory
Number Of Elements, n_{cyl}	2	No	Number of cylindrical element used to create the pipe
Number Of Subelements, n_{i}	3	Yes	Number of integration points on each element
Top Location, $[x_s, y_s, z_s]$	$[1, 1, 1]$ [m]	No	The starting point of the pipe
Bottom Location, $[x_e, y_e, z_e]$	$[0, 0, -5]$ [m]	No	The ending point of the pipe

Ramp Time, T_{R}	5 [s]	Yes	The Morison force is ramped up from 0 to T_{R}
Velocity Field	.current0 [m/s]	No	The current velocity field expressed as a spline function
Current Direction, θ_{c}	$\frac{2\pi}{3}$	Yes	The current propagation direction
Wave Direction, θ_{w}	$\frac{\pi}{9}$	No	The main propagation direction of the waves
Water depth, h	500 [m]	No	The average waterdepth
Wave Period, T	20 [s]	No	The time it takes for a wave to repeat itself
Wave Amplitude, ζ_0	20 [m]	No	Distance from mean surface to the wave crest
Minimum Frequency, ω_{L}	0.2 [1/s]	No	The lower frequency limit in the wave spectrum
Maximum Frequency, ω_{U}	1.6 [1/s]	No	The upper frequency limit in the wave spectrum
Peak Frequency, ω_{P}	0.5	No	The most common wave frequency in the sea state
Alpha, α	0.0081	No	Wave spectrum parameter α in eq 2.7.16
Gamma, γ	3.3	No	Wave spectrum parameter γ in eq 2.7.17
Number Of Waves, $\mathrm{n_w}$	10	No	Number of discretization points in ω-direction in eq 2.7.18
Number Of Directions, $\mathrm{n_d}$	2	No	Number of discretization points in θ-direction in eq 2.7.18
Interval X	$[-10, 10]$ [m]	No	The x range of the visualization area
Interval Y	$[-10, 10]$ [m]	No	The y range of the visualization area
Number Of Plates X, $\mathrm{n_{px}}$	2	No	Number of visualization plates used in x-direction
Number Of Plates Y, $\mathrm{n_{py}}$	2	No	Number of visualization plates used in y-direction

4.2.1 Input parameters

All field boxes except '`Model Name`' are already filled with default values. There are two reasons for this. One of the reasons is to give the user a hint of how the field boxes should be filled in. The other reason is that some parameters need initial values for the underlying macros to run correctly.

Almost all field boxes require single scalar values. '`Model Name`' and '`Velocity Field`' are exceptions since these require the name of the model and the name of the spline function, respectively. The name could either be typed in or selected from a list, the list is shown by double clicking in the field box. '`Top Location`', '`Bottom Location`', '`Interval X`' and '`Interval Y`' are also exceptions, these requires an array as input. '`Top Location`' and '`Bottom Location`' are location coordinates, the coordinates could either be typed in or the coordinates of an existing marker could be selected by double clicking in the field box. 'Interval X' and 'Interval Y' are the intervals in which the wave surface will be visualized, the input must be typed in.

'Velocity Field' need some extra attention, here the current velocity profile described by a spline need to be selected. The x-axis of the spline describes the water depth and the y-axis of the spline describes the current velocity. By default it is filled out with an automatically generated spline called 'current0', the y values in 'current0' are set to zero for all x values, this is equivalent to no current at all. There are two ways to change the current velocity profile, either by modifying the default current profile 'current0' or by replacing it with a new user-defined spline.

'Wave Direction' needs to be expressed in radians if irregular waves are used. If the units are set to radians the underlying macros will assume that the input in 'Wave Direction' is in radians. If the units are set to degrees the input in 'Wave Direction' must be followed by an 'r' for the underlying macros to interpret the input in radians.

After all the input parameters have been inserted a pipe structure can be created by pressing the 'Apply' or the 'OK' button. After the pipe has been created the user might want to change one of the input parameters. Some parameters can be changed without deleting and recreating the pipe, see the design variable column in table 4.2.1. These parameters are set as design variables and can be found in the model tree. To change the parameter value, simply modify the corresponding design variable. If the parameters that are not set as design variables need to be changed, the pipe must be recreated. To simplify the recreation process the 'Regenerate' button could be used after these parameters are changed in the dialog box. By double clicking the 'Regenerate' button a macro that deletes and recreates the pipe will be executed. In the model tree a design variable named 'Dont touch' can be found, within this design variable some necessary internal macro parameters are stored. These are stored here to make the model independent of the macros and they should not be modified.

5 Pipe construction

The user input parameters defined in the dialog box are forwarded to the pipe construction macros. The pipe construction macros is a generic name for a set of macros designed to build a riser pipe. It consists of a main macro that calls the three submacros: '`Offshore_marker`', '`Offshore_cylinder`' and '`Offshore_beam`'. The structure of the pipe construction macros are shown in figure 3.2.1. The following sections will describe how the user input parameters are used to build the pipe. All the input parameters are accounted for in table 4.2.1.

5.1 Main macros

The input parameters are imported into the main macro. First, those parameters which can be changed without rerunning the marcos are set as design variables, see the design variable column in table 4.2.1. If irregular waves are chosen, a wave spectrum, a set of wave amplitudes, wave frequencies, wave numbers and phase displacements need to be calculated. The wave spectrum is obtained from either equation 2.7.16 or 2.7.17 depending on the choice of the spectrum. The wave amplitudes are then calculated by using equation 2.7.15. The parameters used in the equations in this chapter are accounted for in table 4.2.1. The wave frequencies are obtained from equation 5.1.1. The wave numbers are calculated by using equation 5.1.2 assuming deep water condition. The set of phase displacements are randomized values in the interval $[0, 2\pi]$. In addition, if the directional spectrum is chosen, the wave spectrum will be altered according to equation 2.7.18. A set of wave propagation angles will also be created according to equation 5.1.3.

$$\omega_i = \omega_{min} + \frac{(\omega_{max} - \omega_{min})}{n_w}(i - 0.5) \quad \textbf{[5.1.1]}$$

$$k_i = \frac{{\omega_i}^2}{g} \quad \textbf{[5.1.2]}$$

$$\theta_i = \theta_w - \frac{\pi}{2} + \frac{\pi}{n_d}(i - 0.5) \quad \textbf{[5.1.3]}$$

5.1.1 Create markers

The main macro calls upon '`Offshore_marker`', a sub-macro file that creates some basic markers. '`Offshore_marker`' creates the '`ref_sea`'-marker that are placed at the global origin with the global orientations. The x, y-plane of the '`ref_sea`'-marker henceforth defines the mean sea surface. The two markers '`pipe_top`' and '`pipe_bot`' are also created, these define the two ends of the pipe. The created markers can be seen in figure 5.1.1.

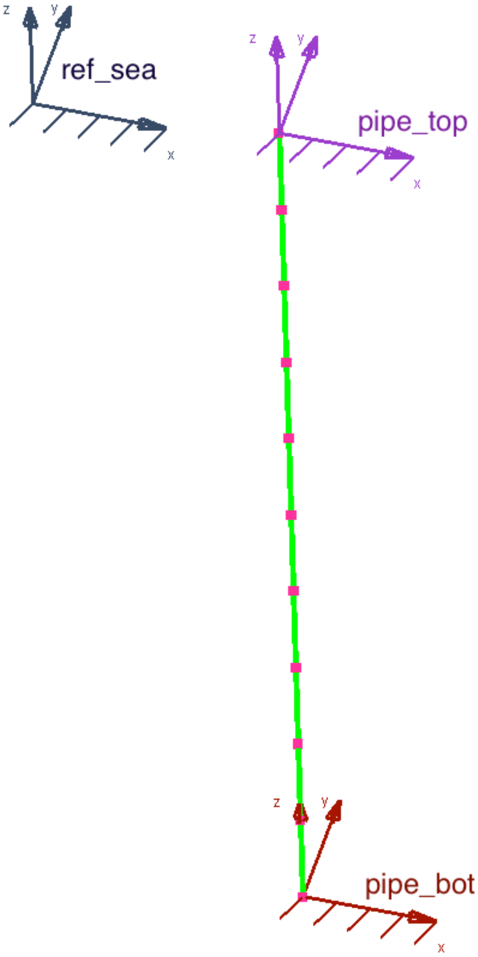

Figure 5.1.1: *Markers created by Offshore_marker*

5.1.2 Create cylindrical elements

The main file then creates the pipe geometry by calling '`Offshore_cylinder`' multiple times. '`Offshore_cylinder`' starts off by creating the local markers '`cyl_top`', '`cyl_bot`' and '`gforce`', according to figure 5.1.2. '`cyl_top`' and '`cyl_bot`' are placed at the center points of the cylinders end. These defines two crucial locations that are later used in the subroutine. The '`cyl_bot`' marker is also used as a reference marker when creating the cylinder geometry. The '`gforce`' marker defines the center of mass and is oriented in the directions of the principal axes of inertia of the cylinder. The mass properties are calculated using ρ_p, ρ_f, r_i, r_o and L, see equations 5.1.8-5.1.11. The mass properties correspond to a pipe with density ρ_p filled with a solid cylinder with density ρ_f. The inertia matrix is expressed in the '`gforce`' marker's coordinate system. No cross terms need to be calculated since these are zero, due to the orientation of the '`gforce`' marker. The appropriate length of the cylindrical elements are calculated utilizing the user specified (x_s, y_s, z_s), (x_e, y_e, z_e) and n_{cyl}, see equation 5.1.12. The specified parameters r_i, r_o and the calculated parameters L, m ,I_{xx}, I_{yy}, I_{zz} are then assigned to the pipe. Finally a general force that calls upon the "`calculation of sea loads`' subroutine is then connected to the '`gforce`' marker, see chapter 6.

$$m_p = (r_o^2 - r_i^2)\pi L \rho_{pipe} \quad \textbf{[5.1.4]}$$

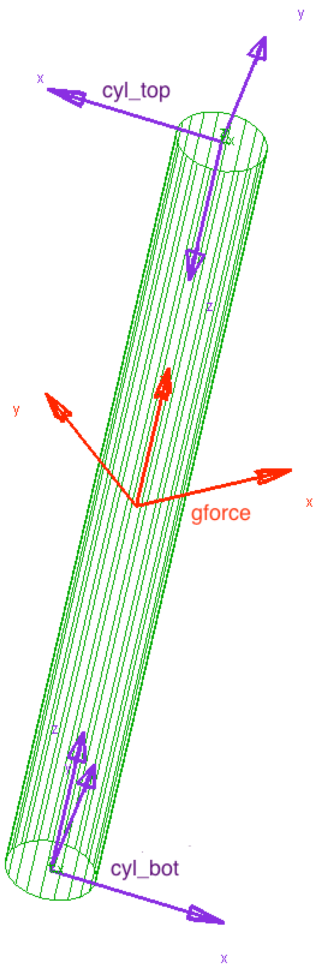

Figure 5.1.2: *The cylindrical element created by Offshore_cylinder*

$$m_f = r_i^2 \pi L \rho_{fluid} \qquad \textbf{[5.1.5]}$$

$$m_{po} = r_o^2 \pi L \rho_{pipe} \qquad \textbf{[5.1.6]}$$

$$m_{pi} = r_i^2 \pi L \rho_{pipe} \qquad \textbf{[5.1.7]}$$

$$m = m_f + m_p \qquad \textbf{[5.1.8]}$$

$$I_{xx} = \frac{1}{4} m_p (r_o^2 + r_i^2) + \frac{1}{12} m_p L^2 + \frac{1}{4} m_f r_i^2 + \frac{1}{12} m_f L \qquad \textbf{[5.1.9]}$$

$$I_{yy} = \frac{1}{4} m_p (r_o^2 + r_i^2) + \frac{1}{12} m_p L^2 + \frac{1}{4} m_f r_i^2 + \frac{1}{12} m_f L \qquad \textbf{[5.1.10]}$$

$$I_{zz} = \frac{1}{2} m_f r_i^2 + \frac{1}{2} m_{po} r_o^2 - \frac{1}{2} m_{pi} r_i^2 \qquad \textbf{[5.1.11]}$$

$$L = \frac{\sqrt{((x_s - x_e)^2 + (y_s - y_e)^2 + (z_s - z_e)^2)}}{n_{cyl}} \qquad \textbf{[5.1.12]}$$

5.1.3 Create beam elements

The main macro then connects the cylindrical elements with flexible Timoshenko beams by calling '`Offshore_beam`' multiple times. '`Offshore_beam`' creates the '`osb_st`' and '`osb_en`' markers at the '`gforce`' marker of cylindrical elements. A beam element between two cylindrical elements can be seen in figure 5.1.3. These markers are oriented with their x-axes parallel to the symmetry axes of the cylinders. A flexible beam element is created between neighboring cylinders '`osb_st`' and '`osb_en`' markers, the x-axes defines the axial direction of the beam element and the y and z axes defines the cross section plane of the beam element. The pipe cross section area and the area of inertia are then calculated using r_o, r_i, see equations 5.1.13-5.1.16. Then all necessary properties are assigned to the beam element, that is the user specified E, G, κ and the calculated A_p, I_{Axx}, I_{Ayy}, I_{Azz}.

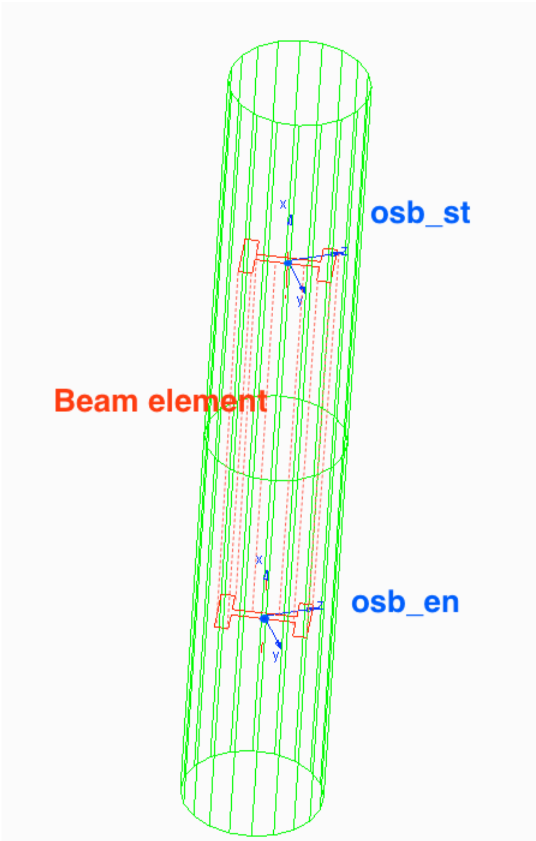

Figure 5.1.3: *The beam and the markers created by Offshore_beam*

$$A_p = \pi(r_o^2 - r_i^2) \tag{5.1.13}$$

$$I_{Axx} = \frac{1}{2}\pi(r_o^4 - r_i^4) \tag{5.1.14}$$

$$I_{Ayy} = \frac{1}{4}\pi(r_o^4 - r_i^4) \tag{5.1.15}$$

$$I_{Azz} = \frac{1}{4}\pi(r_o^4 - r_i^4) \tag{5.1.16}$$

6 Calculation of sea loads

As discussed in section 5.1.2, the riser pipe is made of cylindrical elements. The pipe should be able to interact with a sea environment. To do this, the loads acting on the pipe must be known. The sea loads are therefore calculated in an Adams/Solver subroutine that is called by the cylindrical elements. The subroutine '`Calculation of sea loads`' is programmed in C language. An overview of the subroutine structure is illustrated in the figure 6.0.1 below.

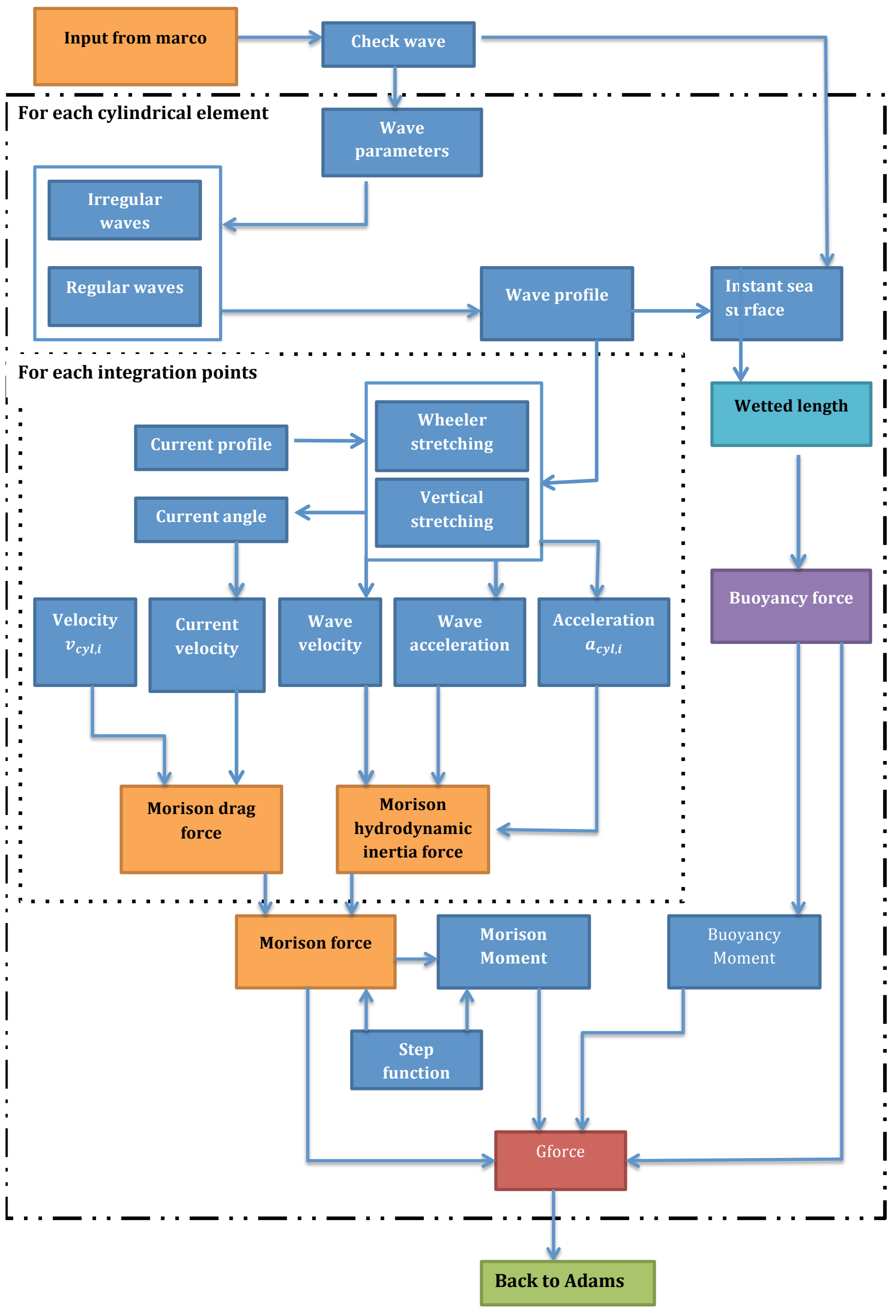

Figure 6.0.1: *Overview of the presented subroutine*

6.1 Buoyancy

This section discusses how the buoyancy load is implemented into the subroutine. A lot of attention is focused on how the buoyancy load is calculated when the cylindrical element is breaking the surface.

6.1.1 Relating cylinder to a sea surface

To calculate the buoyancy force of an object it is crucial to know the position and orientation of objects relative to the sea surface. This master thesis deals only with long and slender cylinders. Based on this fact an approximate position and orientation are calculated by measuring the vertical distance between the cylinder ends centerpoints and the sea surface, see 6.1.1. If the centerpoint of an end is beneath the sea surface the measured value is negative, if it is above the sea surface the measured value is positive. The following definitions are then made:

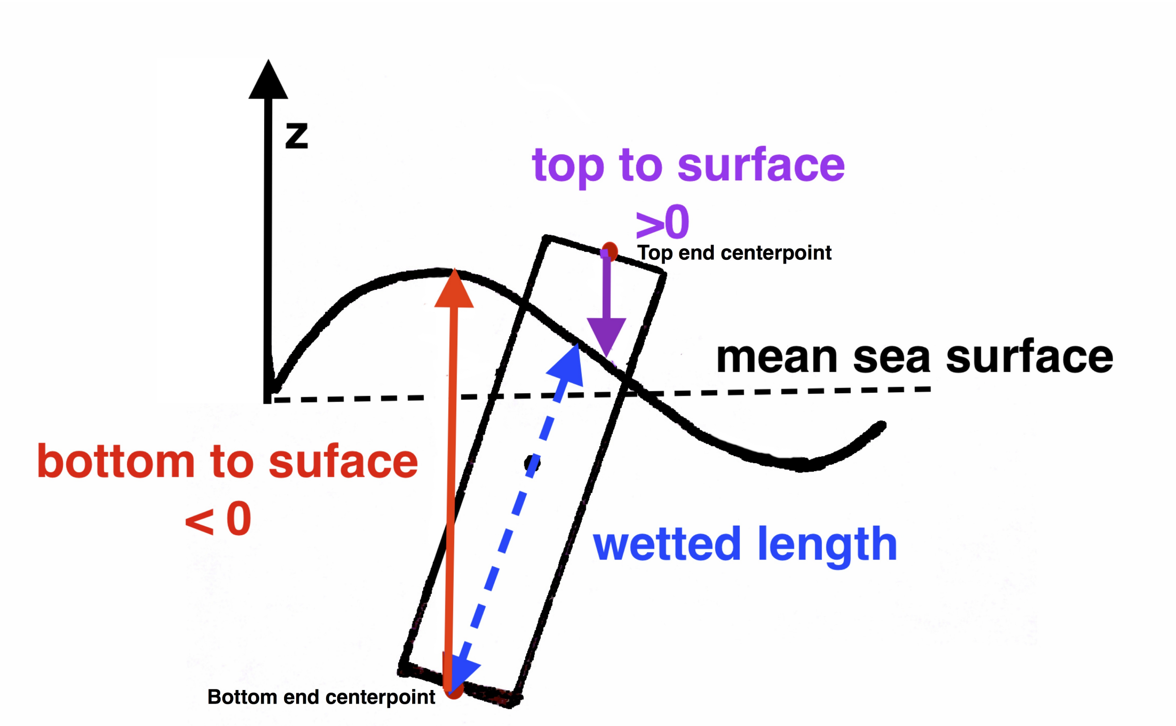

Figure 6.1.1: *Overview of a cylindrical element with important definitions*

Definition 1.

- *If both the measured values are negative, the cylinder is assumed to be fully submerged.*
- *If both the measured values are positive the cylinder is assumed to be fully emerged.*
- *If the measured values have different signs the cylinder is breaking the water surface, see figure 6.1.1.*

6.1.2 The buoyancy force

The buoyancy force is calculated according to Archimedes' principle, equation 2.5.2. To use it the volume of the displaced water must be calculated. This could be troublesome if the cylinder is breaking the surface. However, in this master thesis the cylinders are assumed to be nearly vertically oriented. The displaced water volume could therefore be calculated with equation 6.1.1.

$$V = L_w A_c \qquad [\mathbf{6.1.1}]$$

where:

L_w = wetted length, see definition 2 below
A_c = cylinders cross sectional area

The wetted length is defined as follows:

Definition 2.

- *The wetted length is equal to the length of the cylinder for a fully submerged cylinder.*
- *The wetted length is equal to zero when the cylinder fully emerged.*
- *The wetted length is equal to the distance from the centerpoint of the submerged cylinder end to the water surface, along the cylinder axis if breaking the surface.*

It is straight forward to calculate the wetted length when the cylinder is fully submerged and emerged. However, when it is breaking the surface it is more complicated since the surface is nonlinear. This problem and how it is dealt with is discussed in more detail in section 6.1.4

6.1.3 The buoyancy center

The buoyancy force is acting in the buoyancy center, that should be the center of the displaced water volume. The buoyancy center in the cylinder is assumed to be located on the symmetry axis, half the wetted length from the submerged end, see figure 6.1.1. When the cylinder is fully submerged the buoyancy center will coincide with the center of gravity.

6.1.4 Approximate sea surface

The sea surface is described by one or many sine terms, see equation 2.7.5. In order to calculate L_w in equation 6.1.1 the position where the cylinder symmetry axis intersects the sea surface must be calculated. The symmetry axis could be described with the 3D line equation 6.1.2.

$$\frac{x - x_0}{s_x} = \frac{y - y_0}{s_y} = \frac{z - z_0}{s_z} \qquad [\mathbf{6.1.2}]$$

where:

(s_x, s_y, s_z) = a vector parallel to the symmetry axis
(x_0, y_0, z_0) = a point on symmetry axis

Reordering so that z is alone on the left hand side gives:

$$z = \frac{x - x_0}{s_x} s_z + z_0 \qquad \textbf{[6.1.3]}$$

$$z = \frac{y - y_0}{s_y} s_z + z_0 \qquad \textbf{[6.1.4]}$$

For the intersection point, the z position of the line should be equal to the z position of the wave surface, see equation 2.7.5 . This gives the following nonlinear equation system 6.1.5.

$$f(x,y) = \begin{cases} \frac{x-x_0}{s_x} s_z + z_0 = \sum_{j=1}^{N} \sum_{k=1}^{M} \zeta_{jk} \sin(\omega_j t - k_j x \cos(\theta) - k_j y \sin(\theta) + \epsilon_{jk}) \\ \frac{y-y_0}{s_y} s_z + z_0 = \sum_{j=1}^{N} \sum_{k=1}^{M} \zeta_{jk} \sin(\omega_j t - k_j x \cos(\theta) - k_j y \sin(\theta) + \epsilon_{jk}) \end{cases} \qquad \textbf{[6.1.5]}$$

In general equation 6.1.5 must be solved numerically. In addition the solution might not be unique. To avoid these issues an approximate sea surface is calculated at every time step, see definition 3. In this way an approximate wetted length could be calculated easily through an explicit expression.

Definition 3.
The approximate sea surface is the tangent plane to the sea surface at the (x, y) position of the center of mass of the cylinder.

The tangent plane is described by eq 6.1.6, see [5] for more information about tangent planes.

$$z = \zeta(x_t, y_t) + (x - x_t) \left.\frac{\partial \zeta}{\partial x}\right|_{x_t, y_t} + (y - y_t) \left.\frac{\partial \zeta}{\partial y}\right|_{x_t, y_t} \qquad \textbf{[6.1.6]}$$

where:

$$\frac{\partial \zeta}{\partial x} = -\sum_{j=1}^{N} \sum_{k=1}^{M} \zeta_{jk} k_j \cos(\theta) \cos(\omega_j t - k_j x \cos(\theta) - k_j y \sin(\theta) + \epsilon_{jk}) \qquad \textbf{[6.1.7]}$$

$$\frac{\partial \zeta}{\partial y} = -\sum_{j=1}^{N} \sum_{k=1}^{M} \zeta_{jk} k_j \sin(\theta) \cos(\omega_j t - k_j x \cos(\theta) - k_j y \sin(\theta) + \epsilon_{jk}) \qquad \textbf{[6.1.8]}$$

$(x_t, y_t) = x$, y coordinates of the center of mass of the cylinder

Assume that the axis of symmetry intersects the tangent plane at point $\mathbf{P}$, see figure 6.1.2, the tangent plane is expressed with equation 6.1.9. The axis of symmetry is then expressed using the line equation in vector form, see equation 6.1.10. If point $\mathbf{P}$ is the intersection point, equation 6.1.11 is given by substituting the line equation 6.1.10 into the plane equation 6.1.9. Finally the wetted length L_w can be obtained by equation 6.1.12.

$$\vec{\mathbf{n}} \cdot (\mathbf{P} - \mathbf{P_p}) = 0 \qquad \textbf{[6.1.9]}$$

where

$\vec{\mathbf{n}}$ $= (-\frac{\partial \zeta}{\partial x}|_{x_t,y_t}, -\frac{\partial \zeta}{\partial y}|_{x_t,y_t}, 1)$, normal vector to the tangent plane
$\mathbf{P}_p$ = arbitrary point in the tangent plane
$\mathbf{P}$ = the intersection point

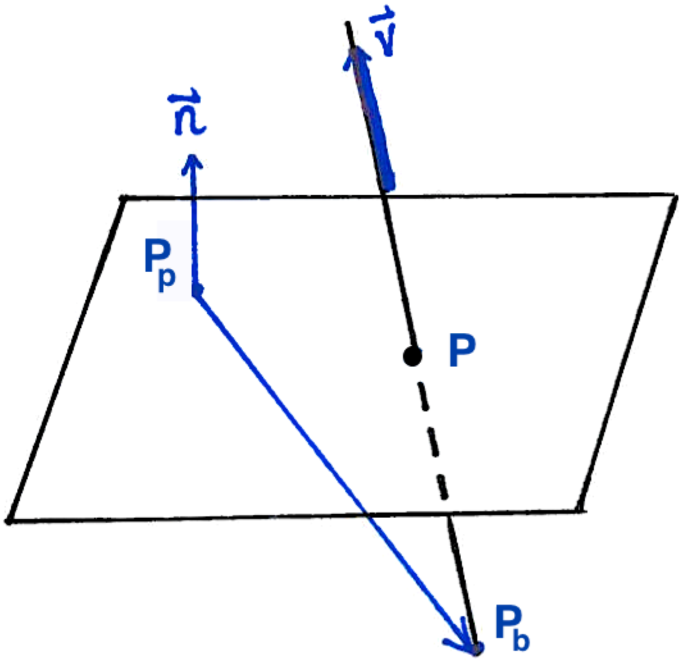

Figure 6.1.2: *The instant sea surface and the symmetry axis intersection point* $\mathbf{P}$

$$\mathbf{P} = \mathbf{P}_b + L_w \cdot \hat{\mathbf{v}} \qquad \textbf{[6.1.10]}$$

where

$\mathbf{P}_b$ = lowest end center point on a cylindrical element
$\hat{\mathbf{v}}$ = unit vector pointing upwards along the axis of symmetry

$$\vec{\mathbf{n}} \cdot (\mathbf{P}_b + L_w \cdot \hat{\mathbf{v}} - \mathbf{P_p}) = 0 \qquad \textbf{[6.1.11]}$$

$$L_w = \frac{\vec{\mathbf{n}} \cdot (\mathbf{P}_p - \mathbf{P}_b)}{\vec{\mathbf{n}} \cdot \hat{\mathbf{v}}} \qquad \textbf{[6.1.12]}$$

When the cylinder symmetry axis is nearly parallel to the tangent plane, $\vec{\mathbf{n}} \cdot \hat{\mathbf{v}}$ becomes small. This might cause numerical issues that lead to unrealistically large L_w values. An extra constraint is therefore introduced so that the wetted length never could be longer than the cylinder length.

6.2 Current

The current profile, the relationship between current velocity and z position, needs to be defined. A one-dimensional current profile is defined by the user with a spline object in Adams. It is assumed that the current profile is uni-directional, that is, the current direction is constant. It is also assumed that the current direction only can vary in the horizontal plane. In this master thesis, the current is assumed to be time independent. The current velocity vector could then be calculated from equation 6.2.1.

$$\mathbf{v}_c = \begin{bmatrix} \cos(\theta_c) \\ \sin(\theta_c) \\ 0 \end{bmatrix} v_{spline} \qquad [\mathbf{6.2.1}]$$

$\mathbf{v}_c$ = Current velocity vector
θ_c = Current propagation direction
v_{spline} = User-defined current profile

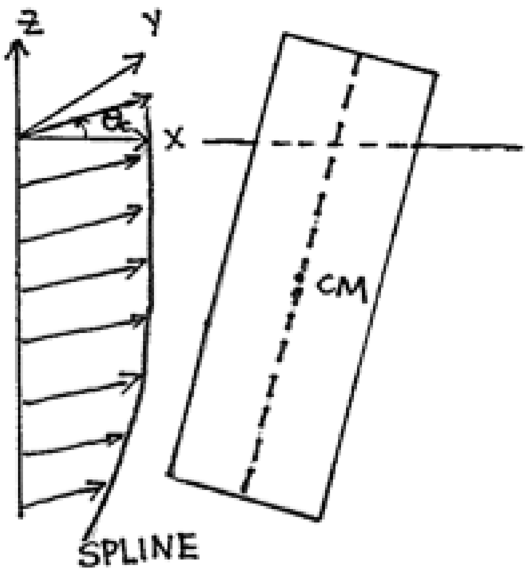

Figure 6.2.1: *The current travelling in direction θ_c*

Since the current velocity field is assumed time independent, the inertia force in Morison's equation due to the current becomes insignificant. The drag force is calculated by numerical integration over the cylindrical element. The number of integration points are specified by the user in the dialog box, see table 4.2.1. The total force on a cylindrical element is calculated by equation 6.2.2:

$$F_{cyl} = \sum_{i=1}^{N} \frac{1}{2} \rho_{sw} C_d A_f dL_i \mathbf{v}_{rn,i} |\mathbf{v}|_{\mathbf{rn,i}} \qquad [\mathbf{6.2.2}]$$

where:

F_{cyl} = Morison force on a cylindrical element
dL_i = length of a subelement i

The relative normal velocity $\mathbf{v}_{r,i}$ is calculated by projecting the relative velocity, obtained by equation 2.2.3, onto the cylinder cross sectional plane. In the subroutine the projection is done by transforming the velocity vector to the '`gforce`' marker coordinate system, then the z component is set to zero and the velocity vector is transformed back to global coordinates. In this case the wave velocity is set to zero so equation 2.2.3 is rewritten to equation 6.2.3.

$$\mathbf{v}_{rn,i} = proj_n(\mathbf{v}_{c,i} - \mathbf{v}_{cyl,i}) \qquad [\mathbf{6.2.3}]$$

The velocities of the current at the integration points, $\mathbf{v}_{c,i}$, are obtained by evaluating the user-defined spline. If constant extension is used the spline is evaluated at the global z-positions of the integration points. If wheeler stretching is used equation 2.7.9 is used to evaluate the spline. Equation 2.1.1 is used to calculate the velocity of the integration point $\mathbf{v}_{cyl,i}$. To do this, the global velocity, $\mathbf{v}_{cm}$ and the global angular velocity, ω, of the bodyfixed '`gforce` ' marker is measured. The coordinate systems are discussed in section 5. The distance from the '`gforce`' marker to the integration point, $\mathbf{r}_{cm->i}$, is also measured in the global coordinates. Then $v_{cyl,i}$ is calculated with equation 6.2.4.

$$\mathbf{v}_{cyl,i} = \mathbf{v}_{cm} + \boldsymbol{\omega} \times \mathbf{r}_{cm\rightarrow i} \qquad \textbf{[6.2.4]}$$

where:

$\mathbf{v}_{cm}$ = the velocity at the center of mass of the cylindrical element
$\mathbf{r}_{cm\rightarrow i}$ = displacement vector from the center of mass for each element to the integration point

The forces on the cylindrical element must be moved to the '`gforce`' marker, see section 5.1.2. A moment must therefore be added for each integration point according to section 2.4. The moment is calculated with equation 6.2.5.

$$\mathbf{M}_{cyl} = \sum_{i=1}^{N} \mathbf{r}_{cm\rightarrow i} \times \mathbf{F}_{cyl,i} \qquad \textbf{[6.2.5]}$$

6.3 Current and waves

If both current and waves are taken into account, all terms must be preserved in Morison's equation. Using numerical integration, the Morison force on a cylindrical element is given by equation 6.3.1.

$$\mathbf{F}_{cyl} = \sum_{i=1}^{N} \left(\frac{\pi}{4}\rho_{sw} D^2 dL_i \mathbf{a}_{wn,i} + \frac{\pi}{4}\rho_{sw} D^2 dL_i C_A \mathbf{a}_{rn,i} + \frac{1}{2}\rho_{sw} C_D D dL_i \mathbf{v}_{rn,i}|\mathbf{v}_{rn,i}|\right) \qquad \textbf{[6.3.1]}$$

The relative normal velocity, $\mathbf{v_{rn,i}}$, is obtained by projecting the relative velocity onto the cylindrical element's cross sectional plane, see equation 6.3.2.

$$\mathbf{v}_{rn,i} = proj_n(\mathbf{v}_{w,i} + \mathbf{v}_{c,i} - \mathbf{v}_{cyl,i}) \qquad \textbf{[6.3.2]}$$

The velocities of the current and the cylinder are discussed in section 6.2. The wave velocity depends on the user-defined wave type, for more information about available wave types, see Chapter 4. If regular deep water waves are used, the velocity components of the waves, $\mathbf{v}_{w,i}$, are given by equation 2.7.1 and 2.7.2. For irregular deep water waves, the directional spectrum, described by equation 2.7.19, can be used to model multi-directional irregular waves. If irregular waves are used without a directional spectrum, the velocity components of the waves, $\mathbf{v}_{w,i}$, are given by equation 2.7.10 and 2.7.11. If a directional spectrum is used, the wave velocities are determined by equation 2.7.20 and 2.7.21.

The fluid normal accelerations and the relative normal accelerations, $\mathbf{a}_{wn}$ and $\mathbf{a}_{rn,i}$, are obtained by projections onto the cylindrical element's cross sectional plane, see equation

6.3.3 and 6.3.4.

$$\mathbf{a}_{wn,i} = proj_n(\mathbf{a}_{w,i}) \qquad \textbf{[6.3.3]}$$

$$\mathbf{a}_{rn,i} = proj_n(\mathbf{a}_{w,i} - \mathbf{a}_{cyl,i}) \qquad \textbf{[6.3.4]}$$

The wave acceleration depends on the user-defined wave type. If regular deep water waves are used, the accelerations of the waves, $\mathbf{a}_{w,i}$, are given by equation 2.7.3 and 2.7.4. If irregular waves are used without a directional spectrum, the accelerations of the waves, $\mathbf{a}_{w,i}$, are given by equation 2.7.12 and 2.7.13. If a directional spectrum is used, the wave accelerations are determined by equation 2.7.22 and 2.7.23. Equation 2.1.2 is used to calculate the cylinder acceleration at each integration point, $\mathbf{a}_{cyl,i}$. To do this, the acceleration at the cylinders center of mass, $\mathbf{a}_{cm}$, the angular velocity and the angular acceleration of the '`gforce`' marker, ω and α respectively, and the distance from the center of mass to the integration point's position, $\mathbf{r}_{cm\to i}$, are measured. The acceleration, $\mathbf{a}_{cyl,i}$, is then given by:

$$\mathbf{a}_{cyl,i} = \mathbf{a}_{cm} + \boldsymbol{\alpha} \times \mathbf{r}_{cm\to i} + \boldsymbol{\omega} \times (\boldsymbol{\omega} \times \mathbf{r}_{cm\to i}) \qquad \textbf{[6.3.5]}$$

The force is moved to the '`gforce`' marker, a moment must be added as in the section 6.2 and can be calculated by equation 6.2.5.

6.4 The subroutine output

After all the sea loads have been calculated, the loads related to the ocean current and the waves are multiplied by a smooth ramp function. The ramp function is introduced to ensure that the initiation phase of the simulation runs smoothly. The loads are stepped from zero to full scale in T_r seconds. All sea loads are then compiled into three force components and three moments and sent back to the cylindrical elements.

7 Wave visualization

In many cases it is convenient for the user to be able to see the waves. An optional wave visualization feature has therefore been added.

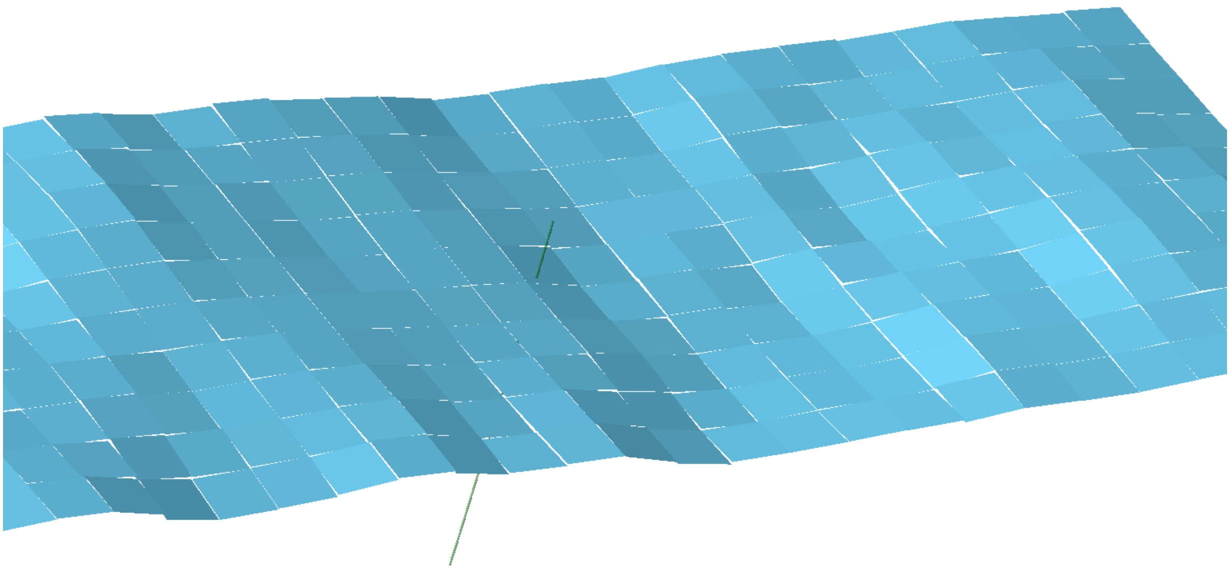

Figure 7.0.1: *The waves visualized with tangent plates*

The motion of the sea surface is visualized with moving rigid body plates, see figure 7.0.1. The sea surface is visualized over the rectangular area specified by the user-defined intervals (x_{min}, x_{max}) and (y_{min}, y_{max}). The intervals are expressed in the global coordinates. The number of plates along the edges of the rectangular area are the user-defined parameters n_{px}, n_{py}. The side length of the plates are calculated with equations 7.0.1-7.0.2.

$$L_{px} = \frac{|x_{max} - x_{min}|}{n_{px}} \qquad \textbf{[7.0.1]}$$

$$L_{py} = \frac{|y_{max} - y_{min}|}{n_{py}} \qquad \textbf{[7.0.2]}$$

The plates used to visualize the sea surface are created by calling '`Wave visualization macro`' multiple times. A single plate is shown in figure 7.0.2. '`Wave visualization macro`' starts off by creating a '`georef`' marker, this is used as reference when creating the plate geometry. Two additional markers at the center of the plate are then created, that is '`mmark`' and '`mmark_refxx`' markers, both has global orientations. The '`mmark`' marker belongs to the plate and the '`mmark_refxx`' marker belongs to the ground. Since there might be many plates and thus many '`mmark_refxx`' markers belonging to the ground, xx in '`mmark_refxx`' represent a unique number used to distinguish between these markers. The motion of the plate is prescribed to the '`mmark`' marker relative to the '`mmark_refxx`' marker and is defined by prescribing the six displacements, here the x, y translation and the z rotation are set to zero. The x, y rotation and the z translation are prescribed with subroutines. The motion of each plate corresponds to the motion of the wave surface's tangent plane at the center of the plate. The z translation is the same as the wave profile at the point motion marker, '`mmark_refxx`' marker. For a regular wave, the value of this point motion can be

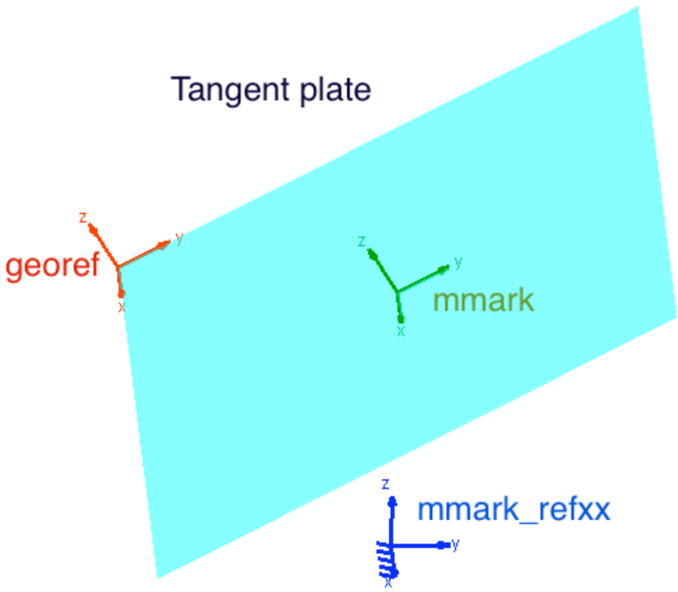

Figure 7.0.2: *A tangent plate*

calculated by using equation 2.7.5. The rotation around the x axis is relatively small and can therefore be approximated by the derivative of the wave profile with respect to y, see equation 7.0.3. In the same way, the rotation around the y axis can be approximated as the negative derivative of the wave profile with respect to x, see equation 7.0.4. For irregular waves, a similar approach is used to determine the x, y rotation and the z translation.

$$\theta_x \approx \xi'_y = -k\sin(\theta)\xi_a \cos(\omega t - kx\cos(\theta) - ky\sin(\theta)) \quad \textbf{[7.0.3]}$$

$$\theta_y \approx \xi'_x = k\cos(\theta)\xi_a \cos(\omega t - kx\cos(\theta) - ky\sin(\theta)) \quad \textbf{[7.0.4]}$$

8 Plug-in

The plug-in is basically a way to package the pipe construction toolkit so that it is easily accessible in Adams/View. In order to do this a library is created, and all macros that are used in the pipe construction toolkit are loaded into that library. The library is then written to a binary file that is moved to the Adams installation folder along with the dll file containing all subroutines. An xml file that defines practical things concerning the plug-in is created and moved to the Adams installation folder. It is defined that it can be accessed in Adams/View only. The plug-in could be accessed under the plug-in ribbon in the '`Offshore`' container, see figure 8.0.1. If the icon is pressed the dialog box will appear.

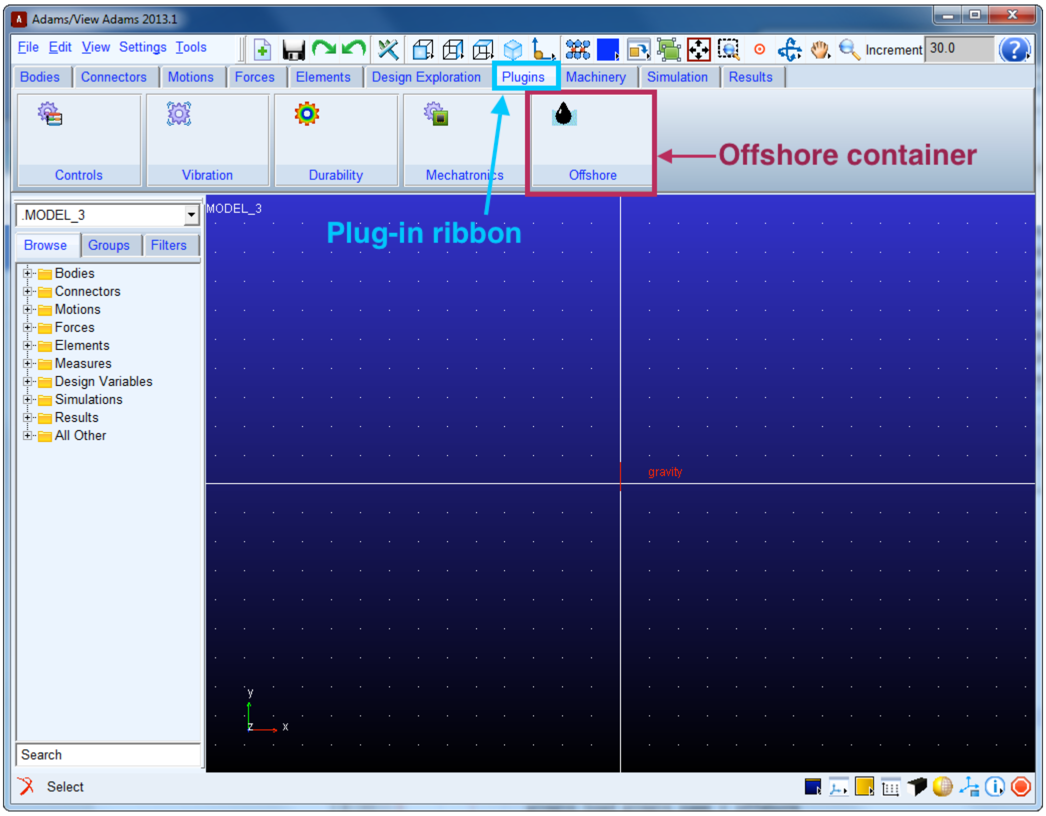

Figure 8.0.1: *A picture of Plug-in ribbon and offshore container*

9 Verification

Now the rise pipe construction toolkit can be accessed as an Adams plug-in. It is important to verify that the models constructed with the toolkit behave realistically. Minor parts of the model like the mass properties are checked by performing simple tests. More crucial parts, like the sea loads calculated in the subroutine, are verified by comparing simulation result from the toolkit to results from other softwares.

9.1 Verification of buoyancy

Two verification cases have been performed to verify the calculated buoyancy load. In the first case results from an Adams simulation was compared to an analytical solution for a vertical cylinder. In the second case, the buoyancy load in the presence of waves was examined.

9.1.1 Case 1. Vertical pipe

In this case, the equation of motion was solved for a vertical pipe. It was assumed that the sea surface was still and that the cylinder was breaking the sea surface at all times. The cylinder was only allowed to move up and down. The forces acting on the cylinder were only gravity and a buoyancy force. An illustration of the described cylinder can be seen in figure 9.1.1.

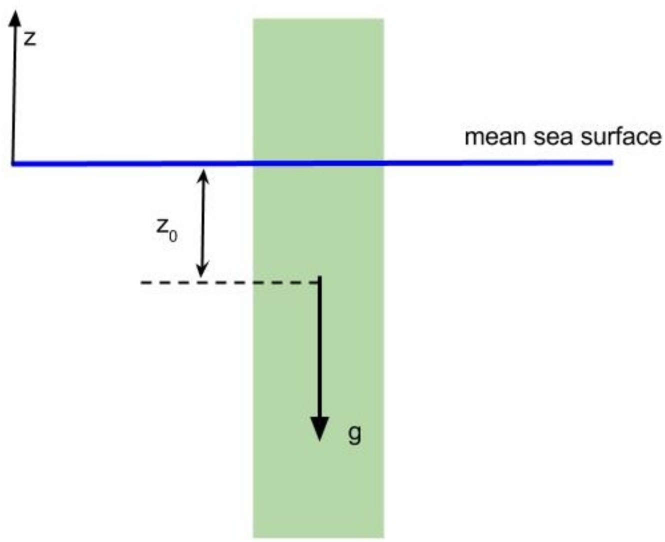

Figure 9.1.1: *A picture of the cylinder used to derive equation 9.1.3*

The equation of motion for cylinder with mass m_c is described by equation 9.1.1 :

$$m_c\ddot{z} - m_c g + \rho_{sw} g A(z + \frac{L_c}{2}) = 0 \tag{9.1.1}$$

where the cylinder is homogeneous with a density ρ_c and has a length L_c, The equation of motion can be rewritten as

$$\ddot{z} + \frac{\rho_{sw} g}{\rho_c L_c} z + (\frac{\rho_{sw}}{2\rho_c} - 1)g = 0 \tag{9.1.2}$$

The differential equation can then be solved by using two initial conditions. When the time is zero, the center of the cylinder is located at a given location, $z(0) = z_0$. The cylinder is also assumed to start from rest, $\dot{z}(0) = 0$. The solution to the differential equation is then given by equation 9.1.3 :

$$z = \left(z_0 - \frac{(\frac{\rho_{sw}}{2\rho_c} - 1)g}{\frac{\rho_{sw} g}{\rho_c L_c}} \right) cos(\sqrt{\frac{\rho_{sw} g}{\rho_c L_c}} t) + \frac{(\frac{\rho_{sw}}{2\rho_c} - 1)g}{(\frac{\rho_{sw} g}{\rho_c L_c})} \tag{9.1.3}$$

The solution was plotted and compared to the simulation result in Adams. The displacements of the center of mass agree with each other, see figure 9.1.2.

Table 9.1.1: The maximum and minimum values in case 1

	Adams	MATLAB
z_{max}	-0.2	-0.2
z_{min}	-0.9250	-0.9249

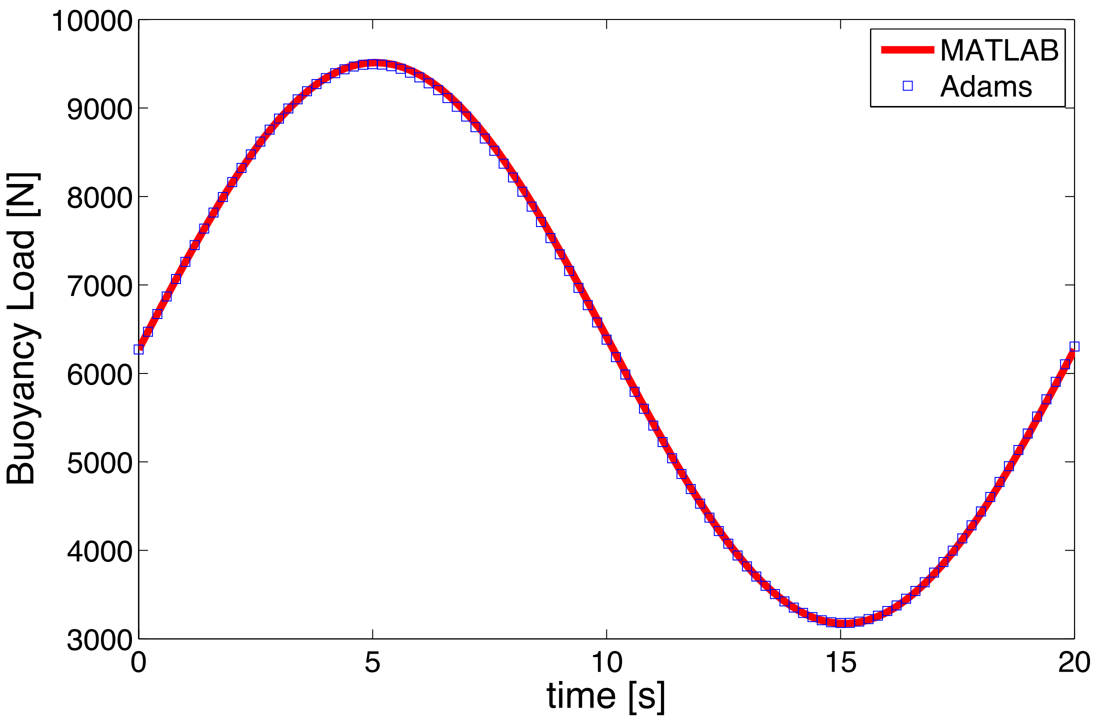

Figure 9.1.2: *Verification of buoyancy for a vertical cylinder, plotted in the interval 0 to 5 seconds*

9.1.2 Case 2. Oblique pipe

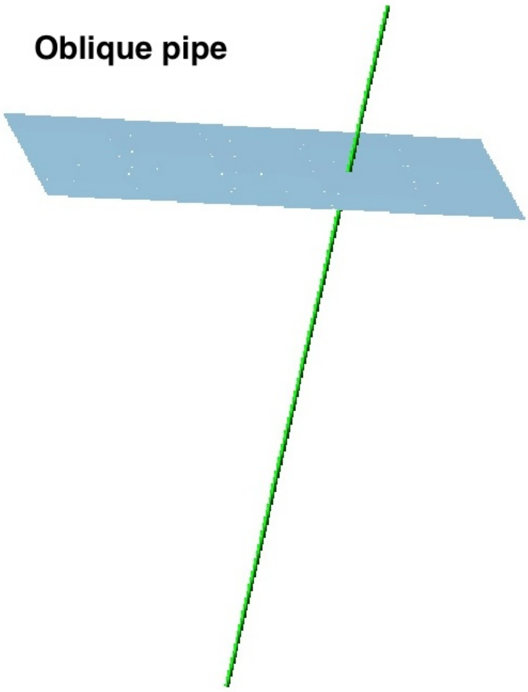

Figure 9.1.3: *A picture of an oblique pipe*

In this case, the approximate sea surface concept discussed in section 6.1.4 was examined. The buoyancy load on an oblique pipe in the presence of regular waves was studied, see figure 9.1.3. A MATLAB code was created to solve the exact wetted length using equation system 6.1.5 for two different set-ups. The difference between the two set-ups is that the oblique pipe in the second set-up was tilted much more than in the first set-up. The set-ups specifications are shown below in table 9.1.2 and table 9.1.3. The results are shown below in figure 9.1.4, 9.1.5 and table 9.1.4.

Table 9.1.2: Buoyancy test Set-ups 1

r [m]	0.1
density [kg/m^3]	1024
Wave amplitude [m]	10
Average waterdepth [m]	1000
Wave period [s]	20
Cylinder top point [m]	(4 -1 15)
Cylinder bottom point [m]	(2 2 -20)
θ_{wave}	50°

Table 9.1.3: Buoyancy test Set-ups 2

r [m]	0.1
density [kg/m^3]	1024
Wave amplitude [m]	10
Average waterdepth [m]	1000
Wave period [s]	20
Cylinder top point [m]	(4 -1 15)
Cylinder bottom point [m]	(100 100 -20)
θ_{wave}	50°

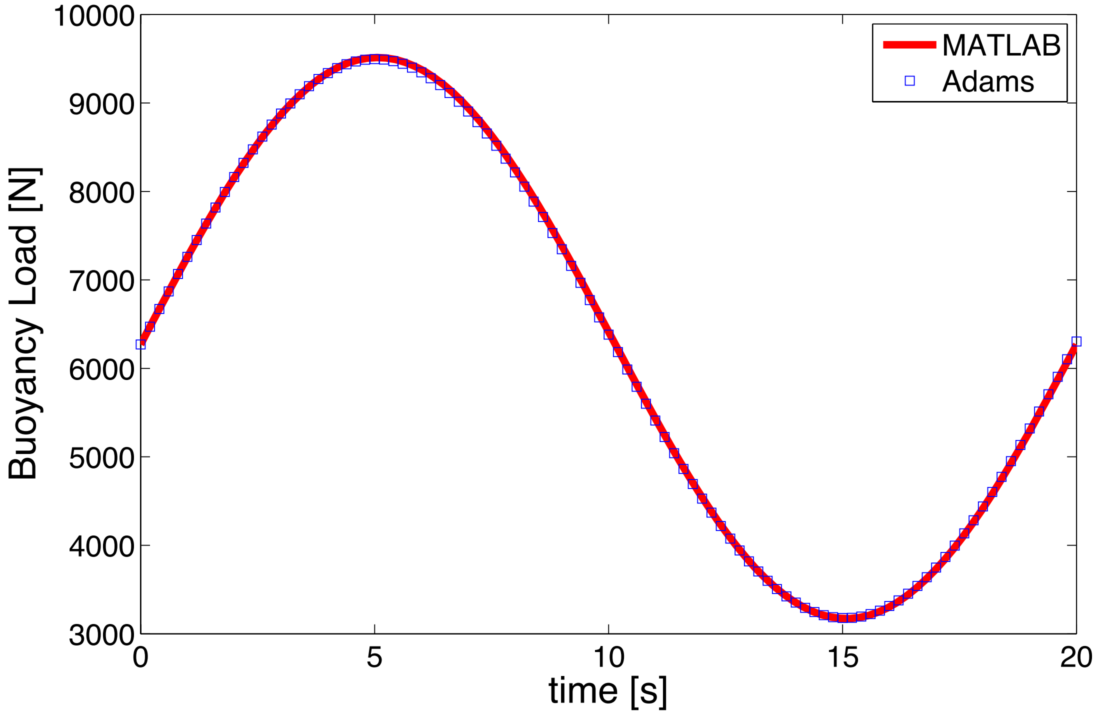

Figure 9.1.4: *The buoyancy load calculated in MATLAB and Adams for set-up 1*

Table 9.1.4: The maximum and minimum values in case 2

	Set-up 1		Set-up 2	
	Adams	MATLAB	Adams	MATLAB
$F_{\text{B,max}}$	9514.7	9513.9	40729	38850
$F_{\text{B,min}}$	3171.4	3171.6	12304	12952

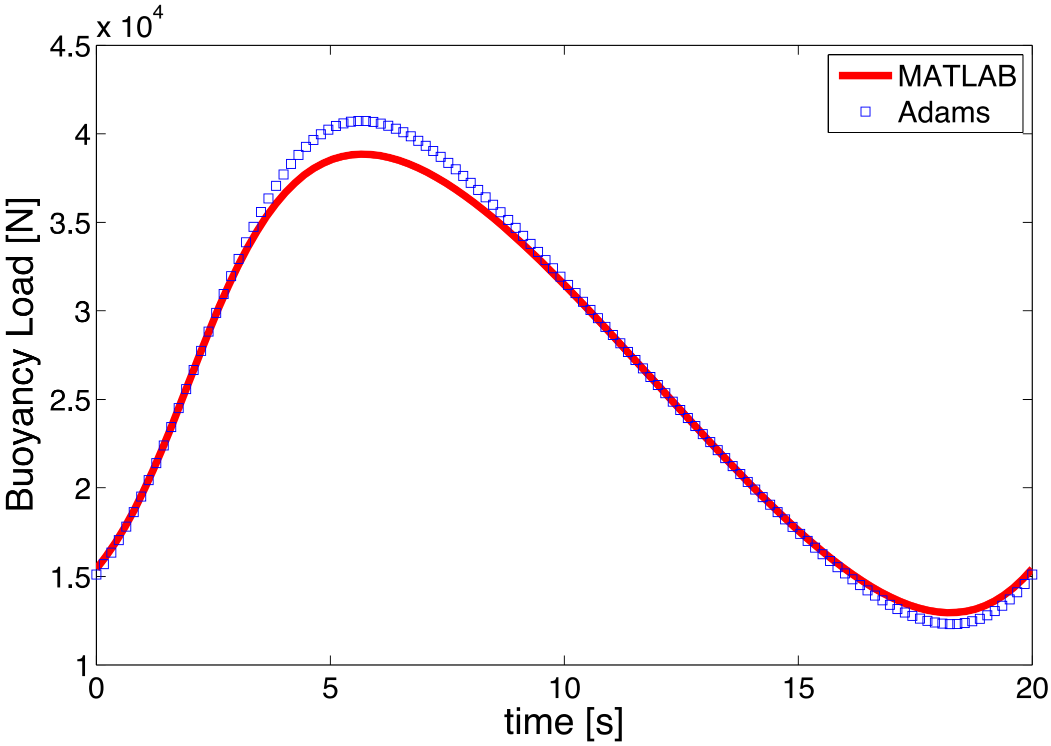

Figure 9.1.5: *The buoyancy load calculated in MATLAB and Adams for set-up 2*

9.2 Comparison with USFOS

To assure that the current and the regular wave functionalities in the pipe construction toolkit work properly, comparisons to the simulation results from the software USFOS was made. The model specifications and the simulation results from USFOS were found in [6]. The riser pipe construction toolkit was used to replicate the models and the simulation results were then compared.

9.2.1 Current verification

In the USFOS theory manual [6] the reaction forces from two simulations of a pipe structure exposed only to an ocean current is presented. One of the simulations was done in USFOS and the other was taken from an Excel macro, that had been used to verify USFOS. In the test the current varied linearly from 1.5 [m/s] at the surface to 0 at the seabed. The pipe was straight and stretching from [30 30 20] to [0 0 -70] in meters. The pipe was also rigid and fixed. The rest of the test parameters used by USFOS are shown in table 9.2.1.

Table 9.2.1: Current load, test parameters

h	70 [m]
D	0.2 [m]
C_{D}	1
C_{M}	0
$\mathrm{N_e}$	1000
$\mathrm{N_{Ie}}$	1000
$\theta_{\mathrm{current}}$	270°

The USFOS report lacks information about some settings. These are obtained by doing some trial and error. It was found that the pipe was massless, no buoyancy exists and the coordinate system was oriented in the same way as the global coordinate system used in this thesis. The test was recreated in Adams with some differences. Since the results seemed to converge after 20 elements and 10 integration points, 1000 elements with 1000 integration points would take unnecessarily long time. So only 100 cylindrical elements with 10 integration points were used instead. The load was ramped up in Adams in order to get a stable initiation process. The time scale in Adams was therefore displaced a few seconds.

Figure 9.2.1 shows the results from USFOS and figure 9.2.2 shows the results from Adams. The maximum and minimum values of the reaction forces from Adams, USFOS and Excel are presented in table 9.2.2.

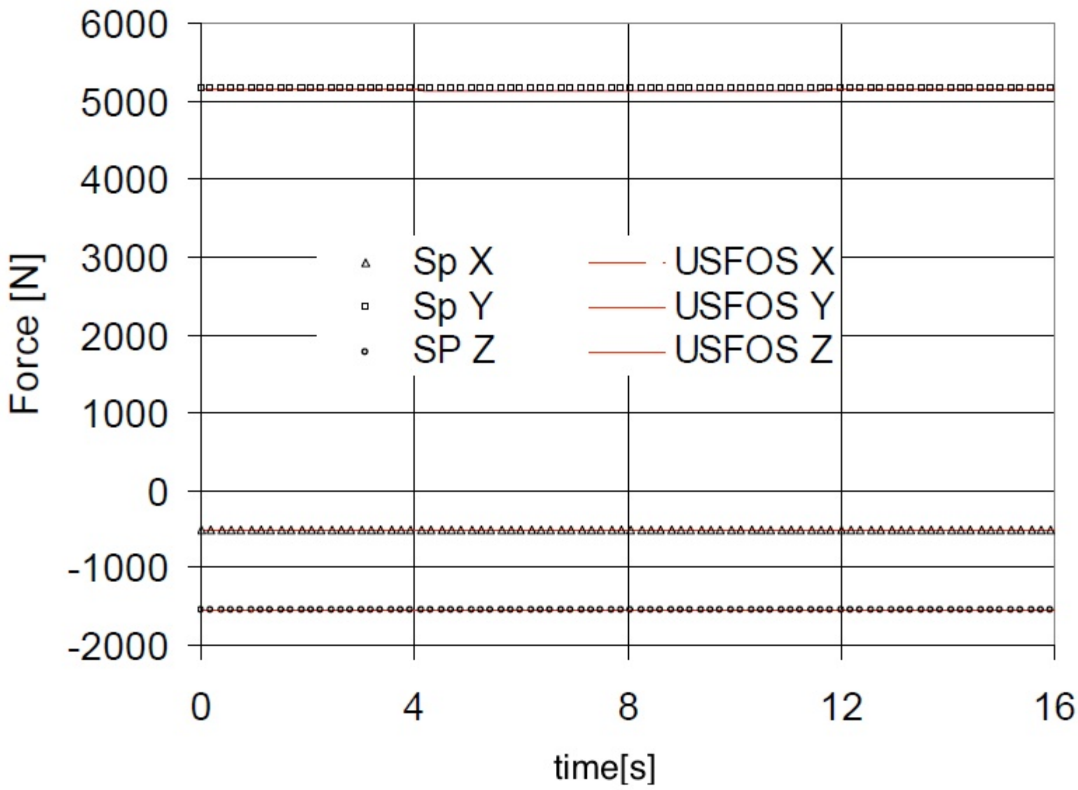

Figure 9.2.1: *The reaction forces due to an ocean current, from the USFOS theory manual*

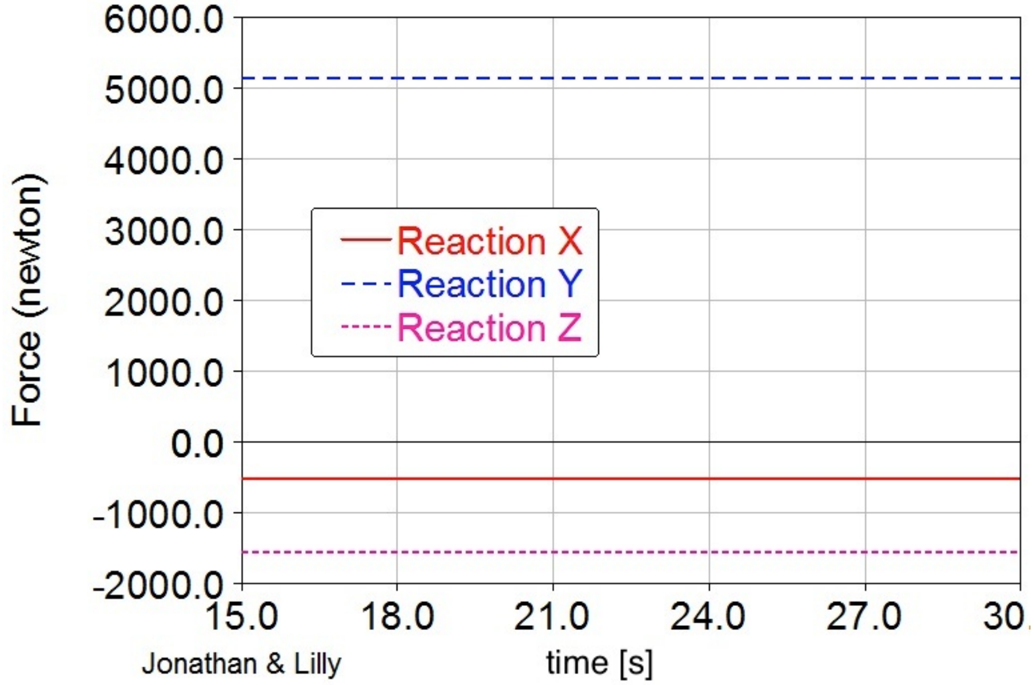

Figure 9.2.2: *The reaction forces due to an ocean current, from the Adams simulation*

Table 9.2.2: Current load, test results

	Adams	USFOS	Excel
R_x	-515.28	-513.98	-515.432
R_y	5148.6	5162.84	5156.3
R_z	-1545.8	-1548.8	-1546.8

9.2.2 Regular wave verification

In the USFOS theory manual [6] the reaction forces from four simulations of a pipe structure exposed only to a regular deep water wave is presented. Two simulations were done in USFOS, one with $C_D = 1$, $C_M = 0$ and one with $C_D = 0$, $C_M = 2$. The other two were done in an Excel macro with the same set-up as in USFOS. The pipe was straight and stretching from [10 10 7] to [0 0 -20] in meters. The pipe was also rigid and fixed. The rest of the test parameters used by USFOS are shown in table 9.2.3.

Table 9.2.3: Wave load, test parameters for the two set-ups

	Set-up 1	Set-up 2
h [m]	70	70
D [m]	0.2	0.2
C_{D}	1	0
C_{M}	0	2
T_{wave} [s]	5	5
ξ_0 [m]	2.5	2.5
$\mathrm{N_e}$	1000	1000
$\mathrm{N_{Ie}}$	1000	1000
θ_{wave} [rad]	0°	0°

As mentioned in section 9.2.1, information about some settings are missing. In addition to those settings already discussed, it was found that constant extension was also used as the extension method, the gravity was assumed to be $g = 9.80655$ m/s^2 and the wave started with the wave crest at the global origin. For the same reason as discussed in section 9.2.1, only 100 cylindrical elements with 10 integration points were used instead. The load was ramped up in Adams in order to get a stable initiation process. The time scale in Adams is therefore displaced one wave period.

Figure 9.2.4, 9.2.6 shows the results from USFOS and figures 9.2.3, 9.2.5 show the results from Adams. The maximum and minimum values of the reaction forces from USFOS and Adams are presented in Table 9.2.4.

Table 9.2.4: Maximum and minimum reaction forces from the regular wave simulations

	$C_{\mathrm{D}} = 1$ Adams	$C_{\mathrm{M}} = 0$ USFOS	Excel	$C_{\mathrm{D}} = 0$ Adams	$C_{\mathrm{M}} = 2$ USFOS	Excel
$R_{x,\mathrm{max}}$ [N]	1463.6	1475.9	1468.0	1662.7	1663.4	1659.0
$R_{x,\mathrm{min}}$ [N]	-5771.5	-5778.3	-5778.1	-1652.6	-1647.3	-1654.7
$R_{y,\mathrm{max}}$ [N]	896.99	905.30	903.04	336.44	336.91	336.46
$R_{y,\mathrm{min}}$ [N]	-812.76	-813.19	-814.67	-720.42	-717.25	-719.78
$R_{z,\mathrm{max}}$ [N]	2154.4	2162.7	2165.2	703.19	704.86	703.99
$R_{z,\mathrm{min}}$ [N]	-586.07	-590.22	-586.40	-566.82	-566.77	-566.73

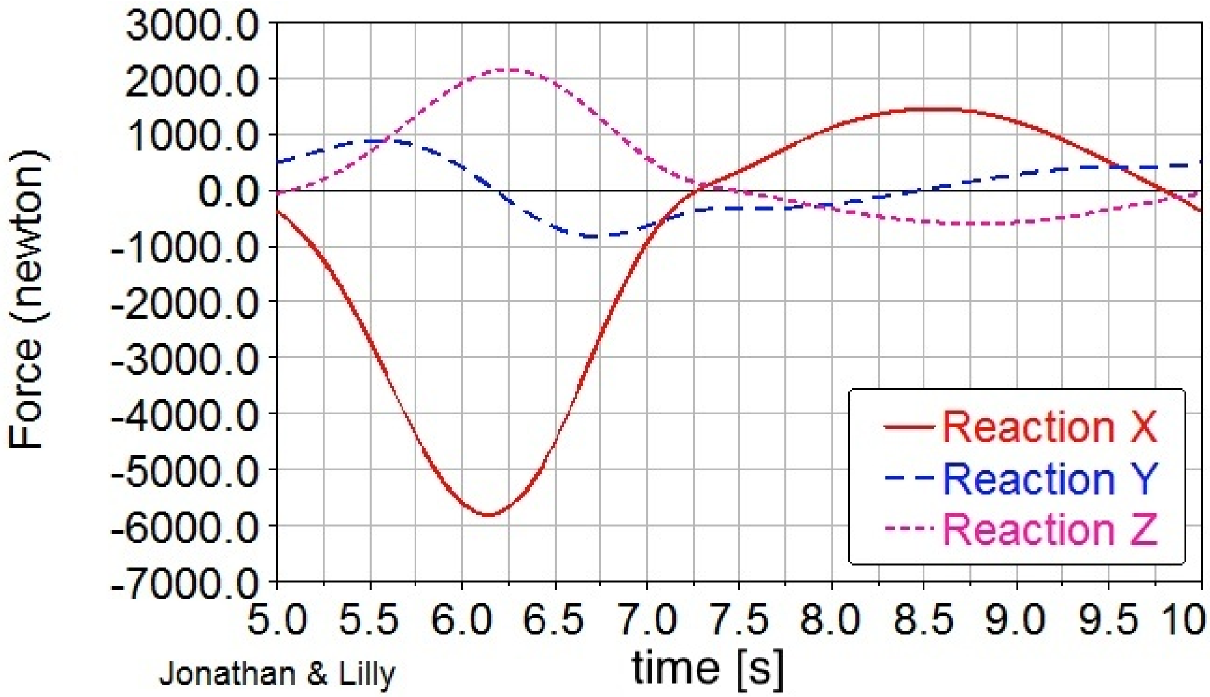

Figure 9.2.3: *The reaction forces in Adams when* $C_D = 1$, $C_M = 0$

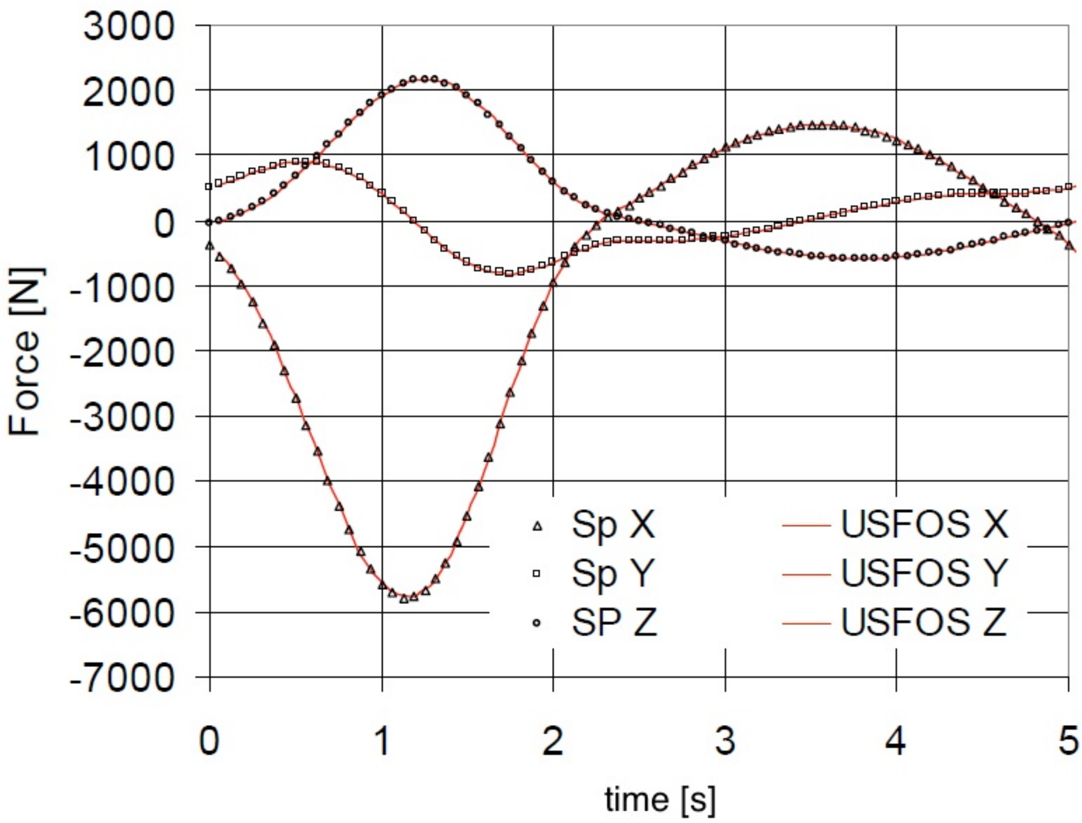

Figure 9.2.4: *The reaction forces from the USFOS theory manual when* $C_D = 1$, $C_M = 0$

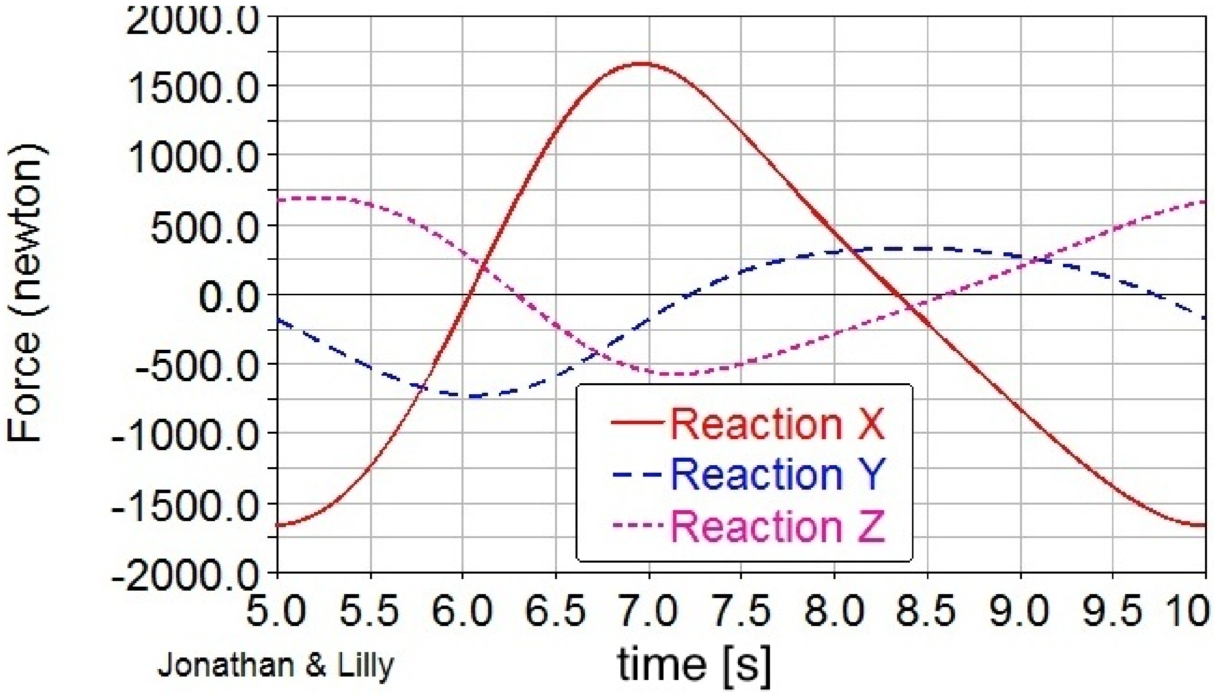

Figure 9.2.5: *The reaction forces in Adams when* $C_D = 0$, $C_M = 2$

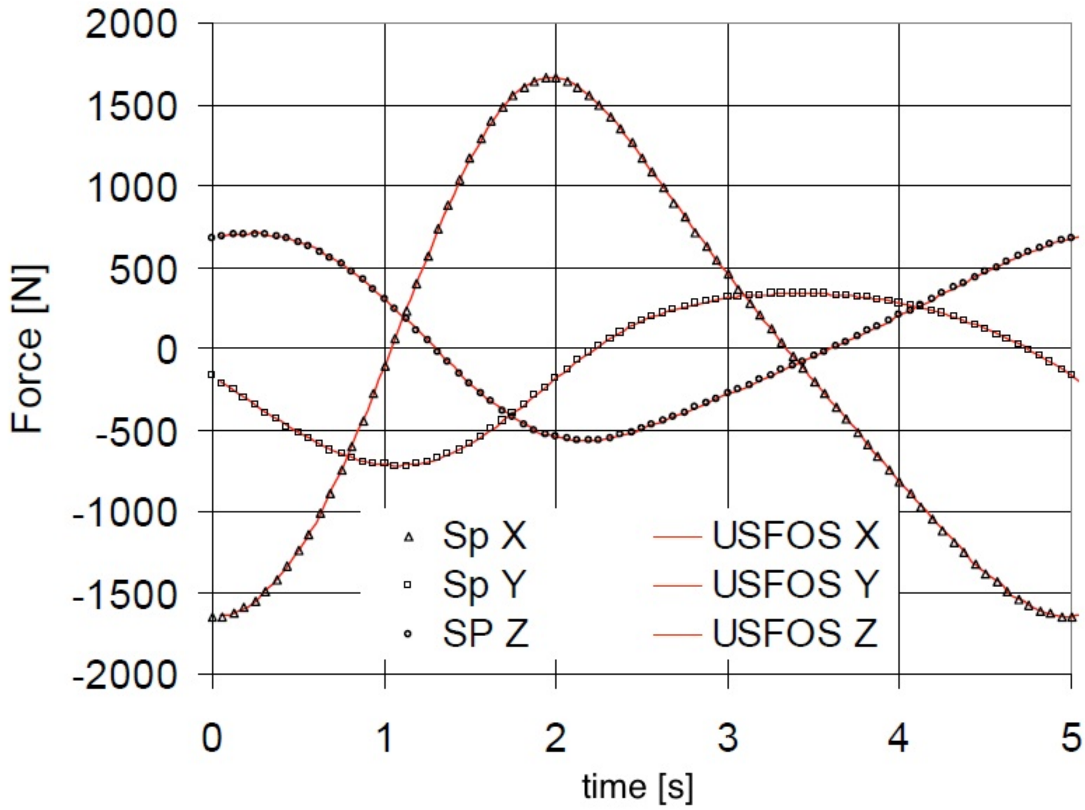

Figure 9.2.6: *The reaction forces from the USFOS theory manual when* $C_D = 0$, $C_M = 2$

9.3 Irregular wave verification

The irregular wave functionality in the pipe construction toolkit was verified by comparing simulation results with OrcaFlex. OrcaFlex is a dynamic simulation software specialized to model offshore structures. Since OrcaFlex requires a license, the OrcaFlex model was built by the company 4Subsea in Norway.

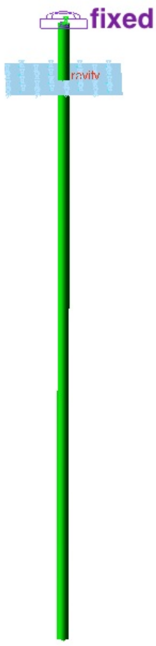

Figure 9.3.1: *A vertical pipe model fixed at the top end with irregular waves*

A vertical riser pipe located in a sea with irregular waves based on the JONSWAP spectrum without a directional spectrum was modelled in both Adams and OrcaFlex, see figure 9.3.1. The upper end of the pipe was fixed and the lower end was free. No current was applied to the model. The pipe was assumed to be rigid. The other parameters used in the model construction are listed below in table 9.3.1. Both simulations were performed in a 1000 s interval with the time step 0.1 s. The output of the simulations were the reaction forces in the fixed joint. Since the waves only propagated in the x-direction and the pipe is vertical, the force components in the y- and z-directions, F_y, F_z, and the torque components around the x- and z-axes, M_x, M_z, were irrelevant. This leaves the force components in x direction, F_x, and the torque component around the y-axis, M_y, to be studied and compared. The simulation results are shown below in figure 9.3.2-9.3.5 and table 9.3.2.

Table 9.3.1: Input for irregular waves verification

Sea environment	
Density seawater [kg/m^3]	1024
Water depth [m]	100
Wave Parameters	
Wave Type	JONSWAP
Number of Components	10
Min frequency [rad/s]	0 - 0.5
Max frequnecy [rad/s]	1.6 - 2
Gamma	3.3
Alpha fetch	0.015
σ_1	7.00E-2
σ_2	0.09
Peak frequency [rad/s]	0.56
Pipe parameters	
Upper end [m]	(0,0,10)
Lower end [m]	(0,0,-100)
Outer diameter [m]	0.35
Inner diameter [m]	0.25
Density pipe [kg/m^3]	7800
C_{D}	1
C_{A}	1

Table 9.3.2: RMS values calculated from OrcaFlex and Adams

	OrcaFlex (10 nodes)	Adams with Adams waves (10 nodes)
F_x [N]	8505.6	6357 - 10713
M_y [Nm]	173560	172160 - 261720

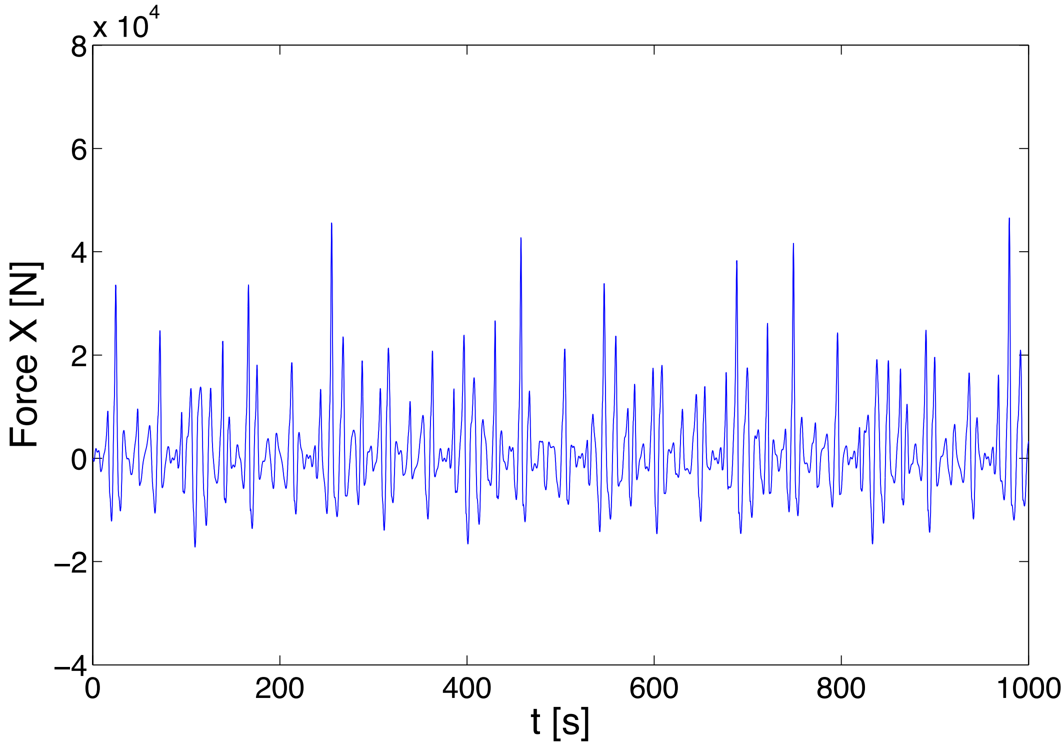

Figure 9.3.2: *The force F_x in Adams with Adams waves (10 nodes)*

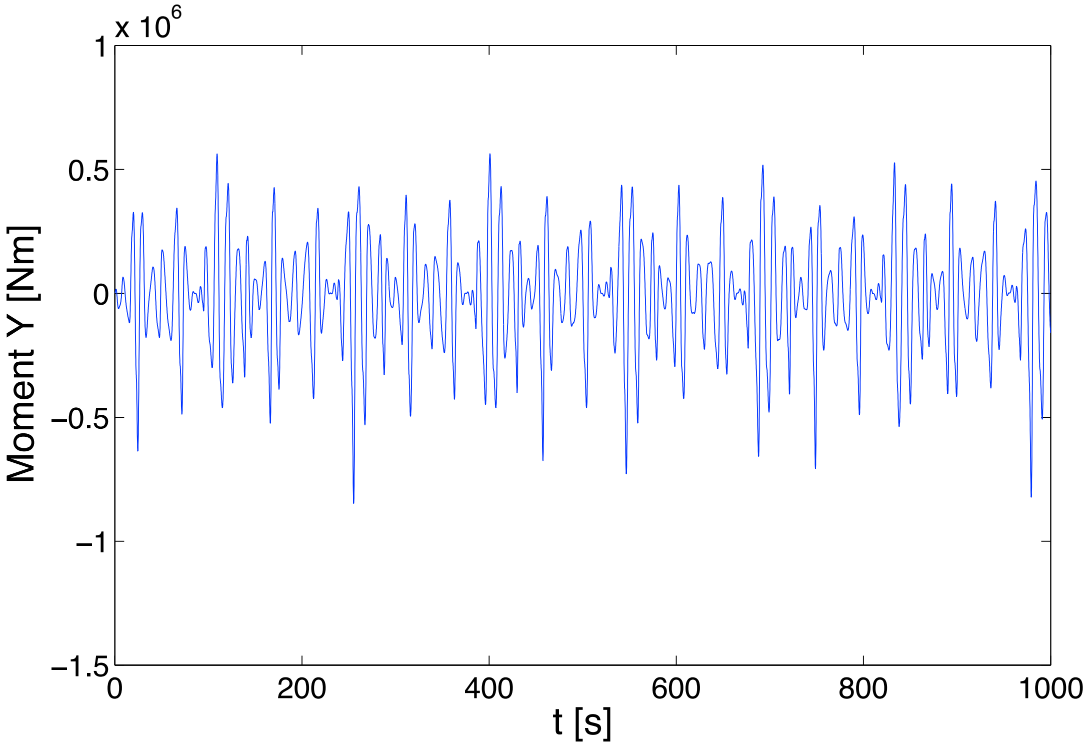

Figure 9.3.3: *The torque M_y in Adams with Adams waves (10 nodes)*

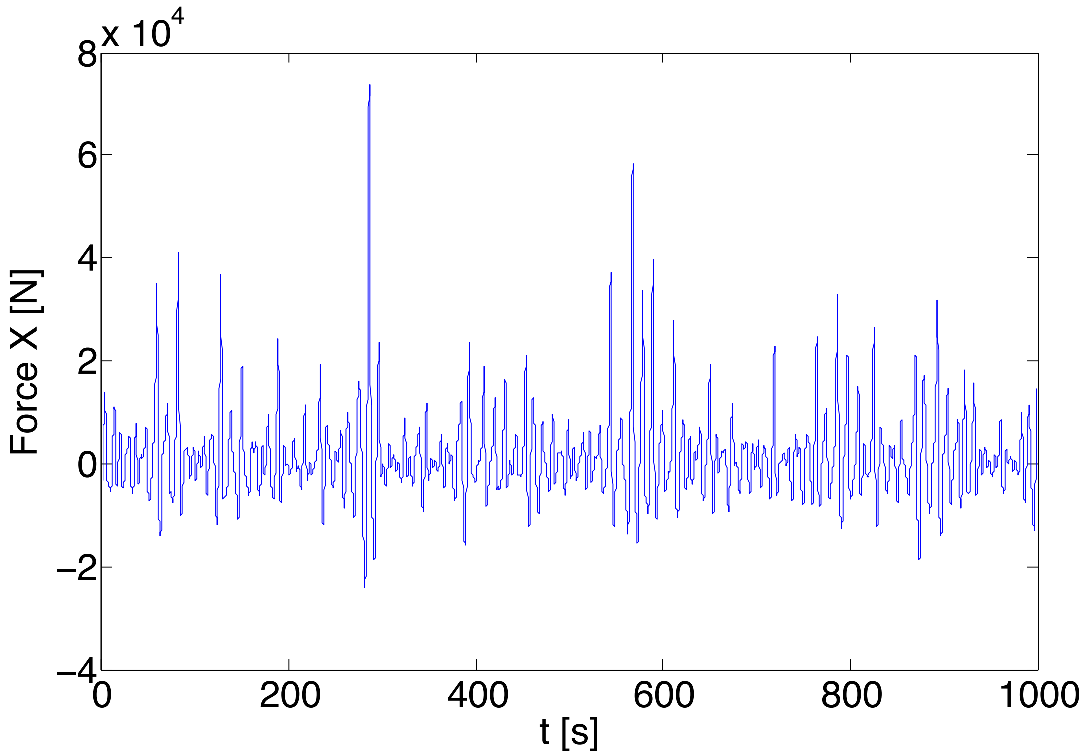

Figure 9.3.4: *The force F_x from OrcaFlex (10 nodes)*

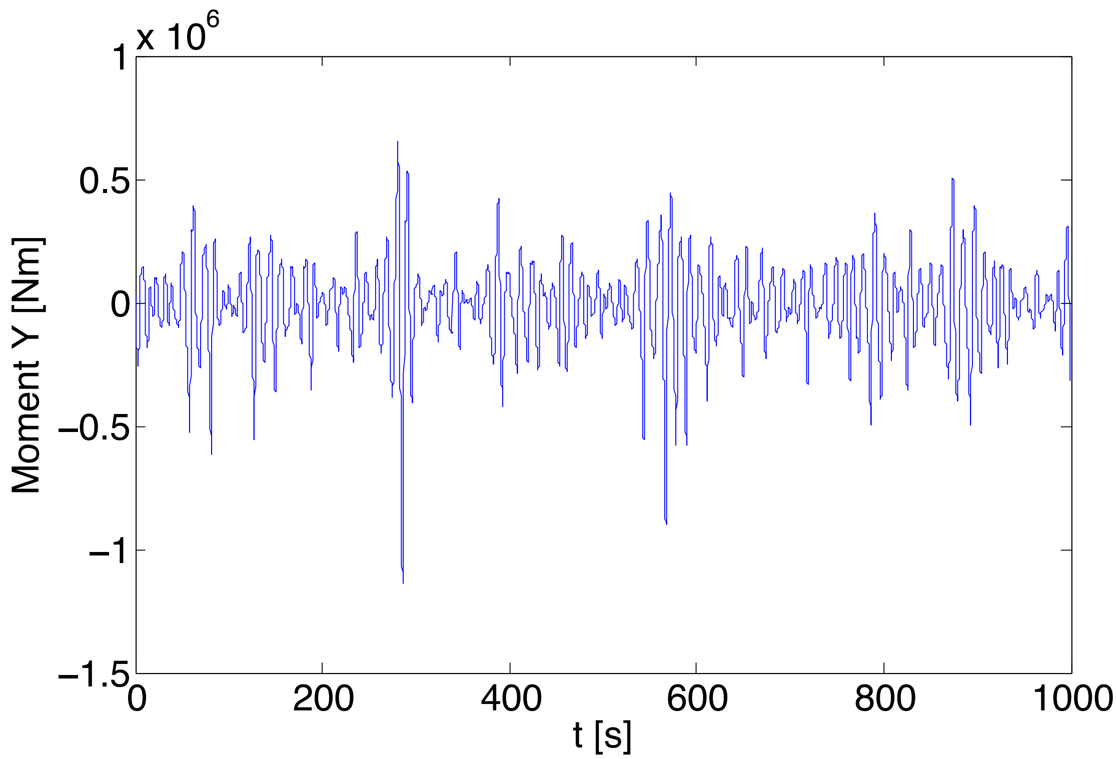

Figure 9.3.5: *The torque M_y from OrcaFlex (10 nodes)*

It can be seen that the results are different in Adams and OrcaFlex. This is because the irregular waves are not the same. There are two reasons for that. The irregular waves are generated by two different approaches in the pipe construction toolkit and in OrcaFlex. The pipe construction toolkit uses the equal frequency spacing approach mentioned in section 2.7.8 when discretizing the wave spectrum. OrcaFlex on the other hand uses the equal energy. In addition, randomized phase displacements are used in both programs when creating the wave components. To be able to compare the result sets Root Mean Square values, so called RMS values, are calculated and shown in table 9.3.2. Since only ten wave components are used, the RMS values will be depending on the interval in which the wave spectrum is discretized. The RMS values will also be depending on the random phase displacements. Therefore RMS values from Adams in table 9.3.2 are given in intervals. The intervals have been obtained by running many simulations with different phase displacements and different minimum and maximum frequencies.

Table 9.3.3: Wave components used in OrcaFlex

Component Frequency (Hz)	Amplitude m	Phase Lag rad	Wave number 1/m	Direction (deg)
7.4159E-2	0.94860	1.3570	2.2625E-2	0
8.2427E-2	0.94860	4.1351	2.7572E-2	0
8.6364E-2	0.94860	8.9834E-2	3.0171E-2	0
8.9333E-2	0.94860	3.2883	3.2228E-2	0
9.2326E-2	0.94860	2.6988	3.4386E-2	0
9.6037E-2	0.94860	2.8369	3.71730E-2	0
0.10197	0.94860	0.87264	4.1874E-2	0
0.11308	0.94860	2.1861	5.1487E-2	0
0.13182	0.94860	4.7597	6.9954E-2	0
0.17733	0.94860	3.0745	0.12659	0

It is hard to verify the calculation of the wave loads when the waves are different. To make the results more comparable, the wave components used in OrcaFlex, listed in table 9.3.3, were inserted into Adams. The simulation results are shown in figure 9.3.6 and 9.3.7. To make a better comparison, the simulation results for the interval between 0 s and 100 s are plotted together, see figure 9.3.8, 9.3.9 and table 9.3.4.

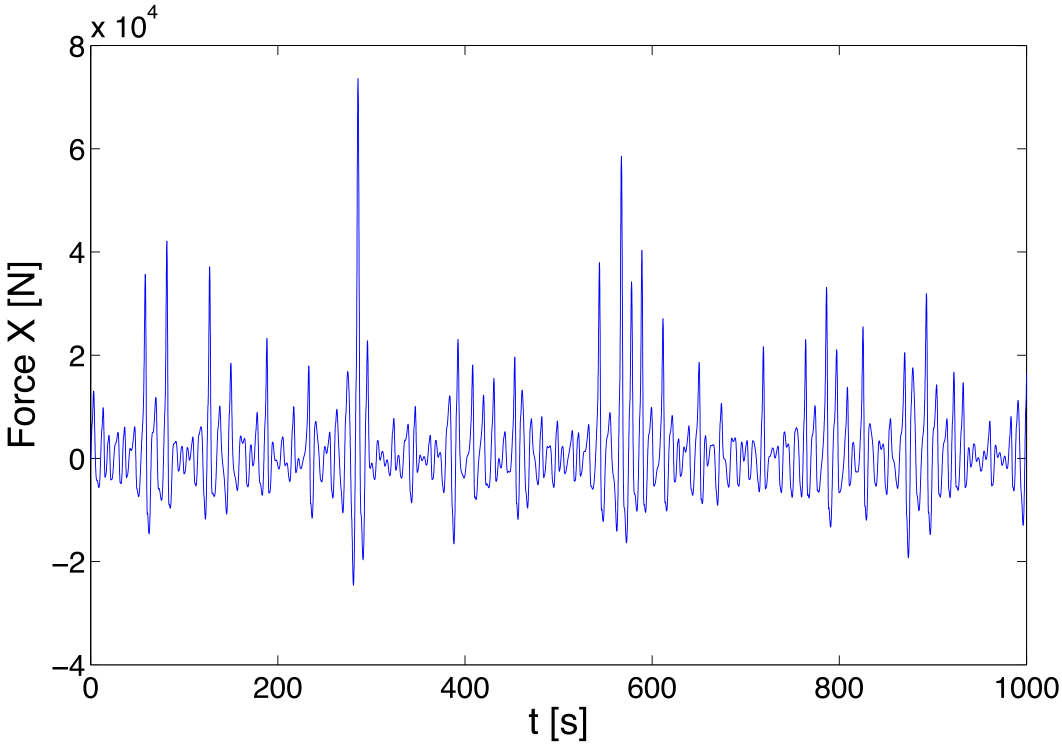

Figure 9.3.6: *The force F_x from Adams with OrcaFlex waves (10 nodes)*

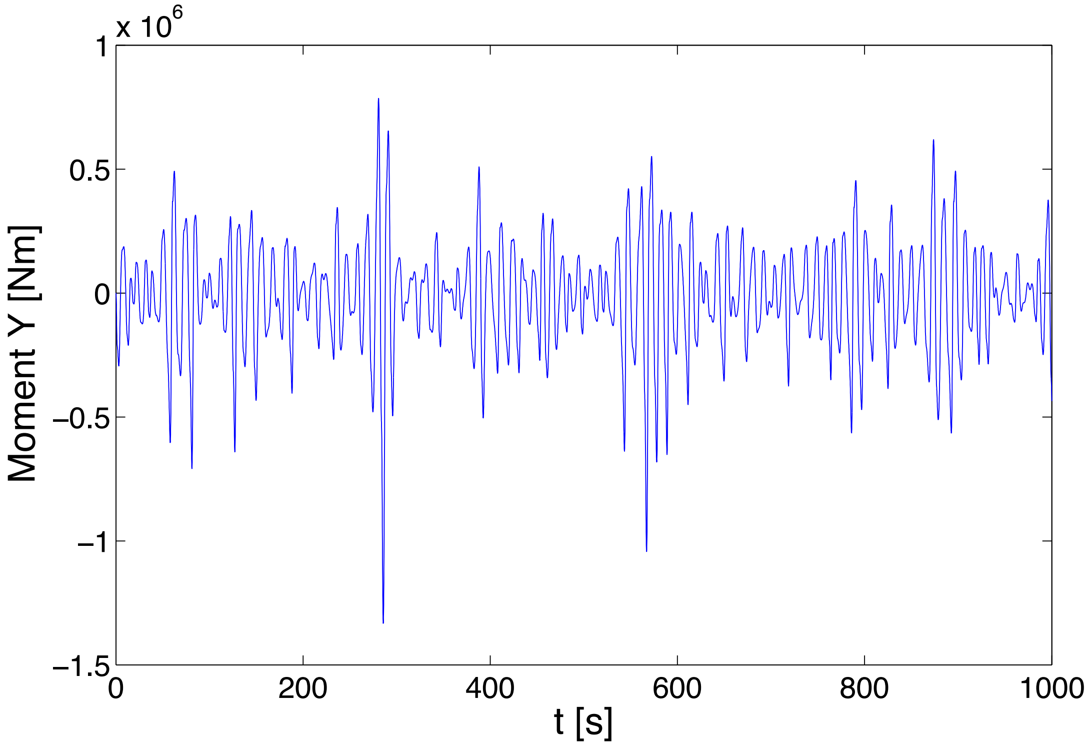

Figure 9.3.7: *The torque M_y from Adams with OrcaFlex waves (10 nodes)*

Table 9.3.4: RMS values calculated from OrcaFlex and Adams with OrcaFlex waves

	OrcaFlex (10 nodes)	Adams with OrcaFlex waves (10 nodes)
F_x [N]	8505.6	8472
M_y [Nm]	173560	213050

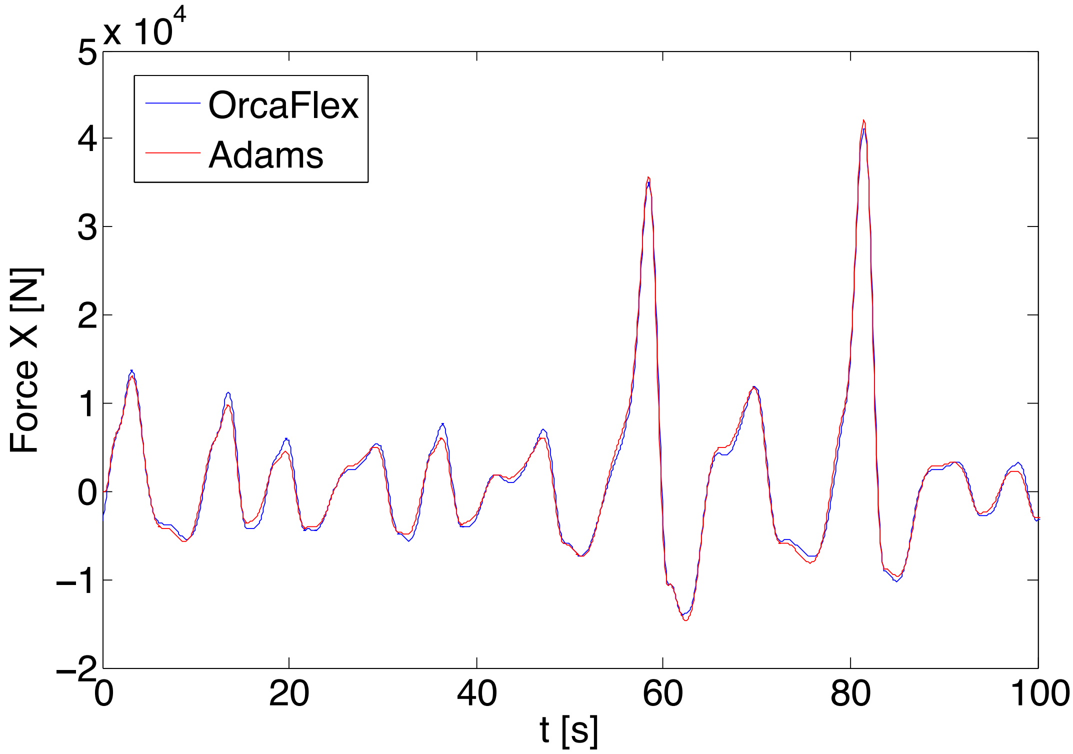

Figure 9.3.8: *A comparison of the forces F_x from OrcaFlex and Adams with OrcaFlex waves, 10 nodes each*

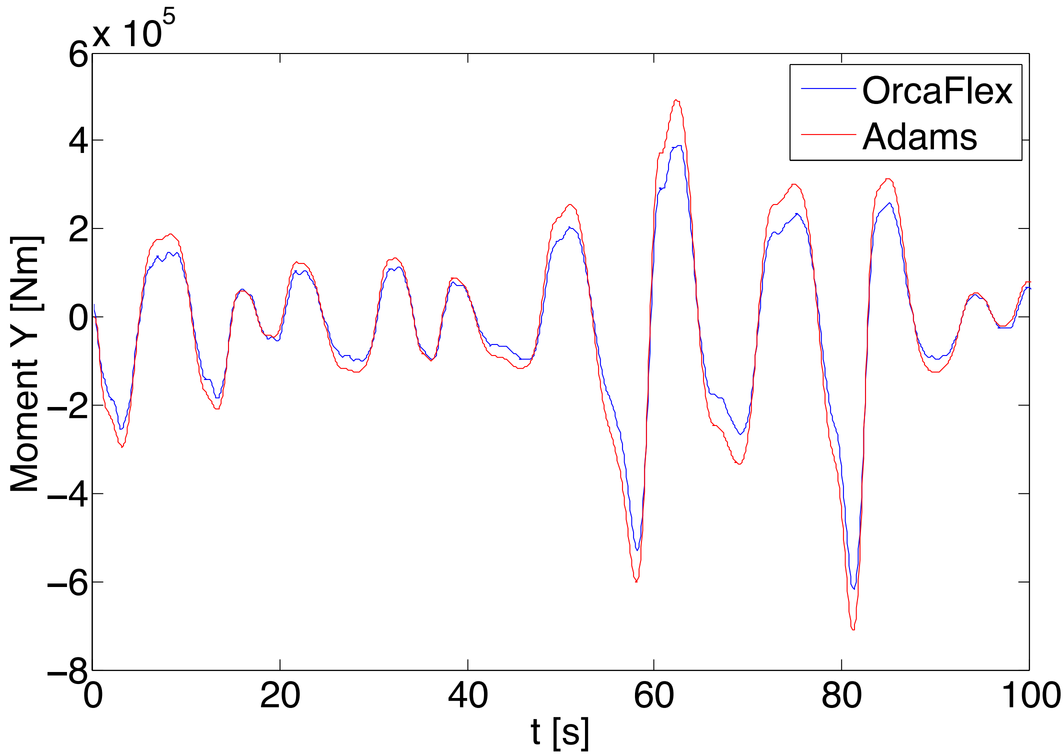

Figure 9.3.9: *A comparison of the torques T_y from OrcaFlex and Adams with OrcaFlex waves, 10 nodes each*

Looking at figure 9.3.8 and 9.3.9, it can be seen that the forces agrees very well, while the moment in OrcaFlex is consistently slightly lower than the moment in Adams. That is very strange since the forces and the moments are closely related. In order to make a well-founded conclusion the moment need to be examined further. To do this, a MATLAB program that model a vertical pipe according to the specifications in table 9.3.1 was created. The wave components generated by OrcaFlex, table 9.3.3, was used. When testing the MATLAB program it was noticed that the results still depended on the number of nodes. Therefore 1000 nodes was used in MATLAB, the Adams model with the OrcaFlex waves was also re-simulated with 1000 nodes to make sure that the model results had converged. The response from the MATLAB simulation is shown in figure 9.3.10 and 9.3.11. The RMS values from both MATLAB and the new Adams simulation are shown in table 9.3.5.

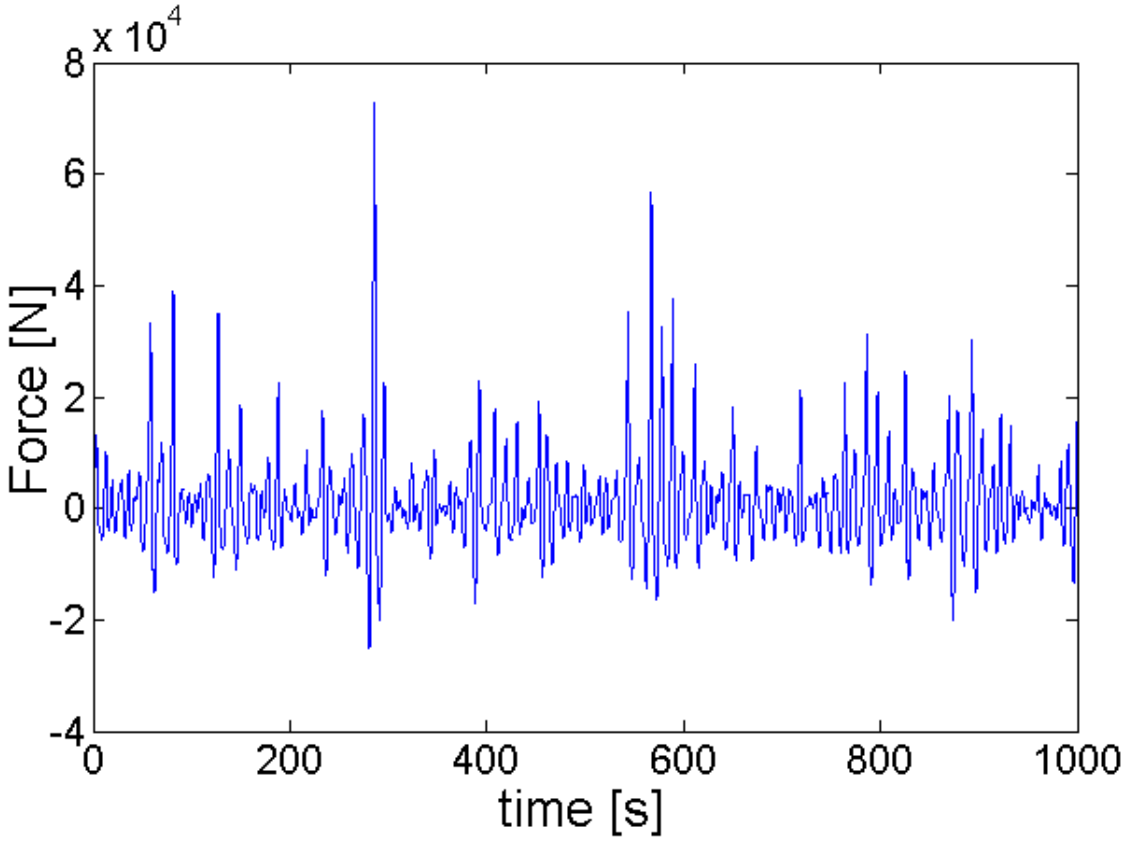

Figure 9.3.10: *The force F_x from MATLAB with OrcaFlex waves (1000 nodes)*

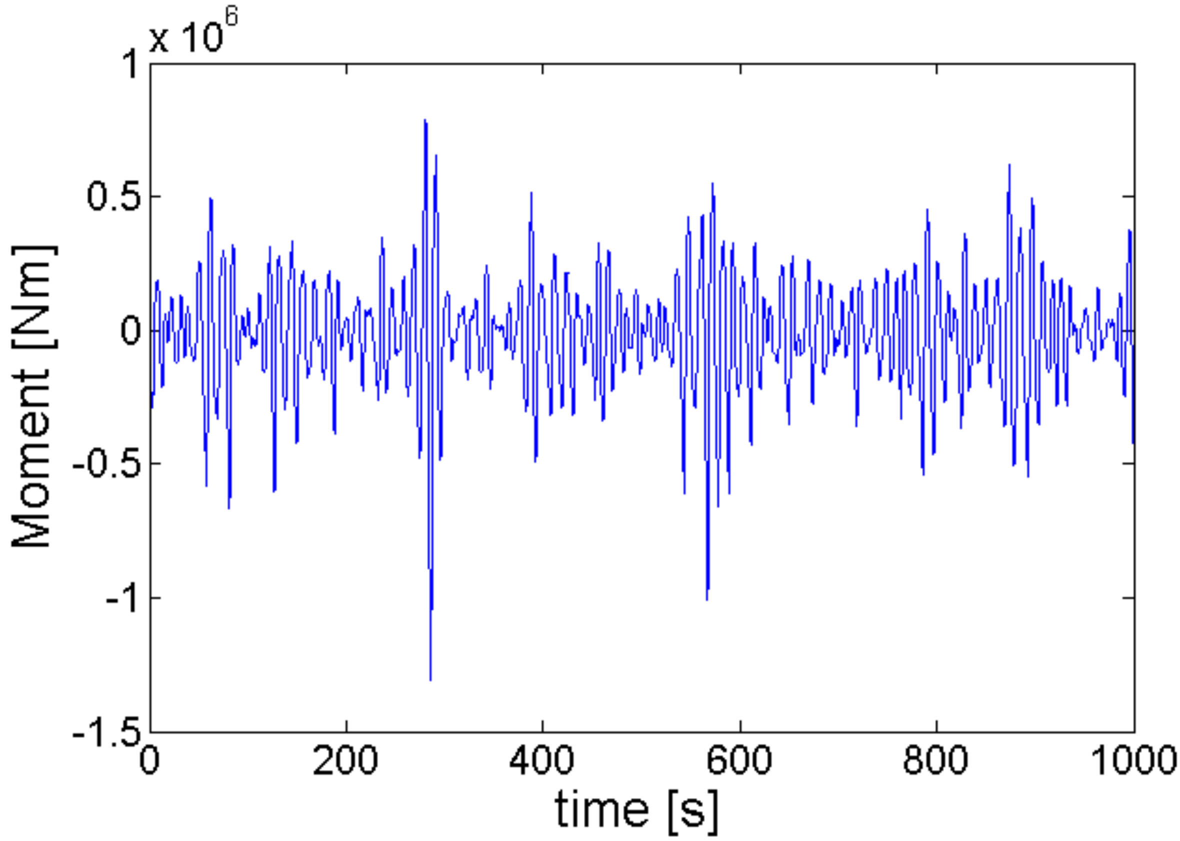

Figure 9.3.11: *The torque M_y from MATLAB with OrcaFlex waves, (1000 nodes)*

Table 9.3.5: RMS values calculated in MATLAB and Adams with OrcaFlex waves with 1000 nodes compared to the results from OrcaFlex with 10 nodes

	Adams with OrcaFlex waves (1000 nodes)	MATLAB with OrcaFlex waves (1000 nodes)	OrcaFlex (10 nodes)
F_x [N]	8386.3	8398.6	8505.6
M_y [Nm]	210410	210780	173560

10 Conclusion and discussion

Considering the verification results in section 9.1, the results suggest that the buoyancy force is correctly calculated. Due to the instant sea surface approximation, the buoyancy force on a pipe that breaks the surface is most accurately calculated when the pipe is close to upright. In section 9.1.2 it is shown that the largest error deviation is approximately 5 percents when the pipe is tilted 75 degrees from the upright position. When the pipe is tilted 6 degrees the error is negligible. These results should only be considered as approximate error estimations. Except for the tilt angle, the error will also vary depending on the wave set-up and the length of the cylindrical element. As a rule of thumb the cylindrical element should never be longer than one quarter of the wavelength. It should be stressed that in a riser pipe model there are only a few cylindrical elements that will break the surface. The majority of the elements will be either fully emerged or fully submerged. Since the buoyancy force calculation will be correct for those elements the total error will be small. Consequently, there is little to gain by improving the buoyancy calculations for a cylindrical element that breaks the surface.

The results in section 9.2 suggests that the loads due to currents and regular waves have been calculated correctly. Neither of the graphs in that section display any noticeable difference between the results from Adams, USFOS and Excel. In table 9.2.2 and 9.2.4 it could be seen that the maximum and minimum values of the reaction forces deviates a little bit. However, the results from Adams are within the deviation range between the USFOS and Excel results. The small deviation could depend on different solver settings, it could also depend on the gravity constant that was assumed due to the lack of information. The verification described in this section was done for specific set-ups. As a consequence there are still functionalities related to both currents and regular waves left to be verified.

Compare figures 9.3.2 to 9.3.4 and figures 9.3.3 to 9.3.5, they are very different. In table 9.3.2 the corresponding RMS values are presented. The RMS value of the force from OrcaFlex is within the RMS range from Adams. The RMS value of the reaction moment M_y in OrcaFlex is just within the RMS range from Adams. This suggests that the irregular waves generated with equal frequency spacing in Adams are comparable to those generated with the equal energy approach in OrcaFlex. In figures 9.3.6 and 9.3.7, the irregular waves generated in OrcaFlex have been used in Adams. Comparing with figures 9.3.4 and 9.3.5 is hard to see any noticeable difference. A closer comparison could be made by looking at figure 9.3.8 and 9.3.9. The reaction forces are very similar while the reaction moment from OrcaFlex seems to be consistently lower than that from Adams. The RMS values in table 9.3.4 suggest the same thing. Since table 9.3.5 shows that the results from the MATLAB model converge towards the same values as the Adams model, it indicates that the moment in Adams is correct. It is possible that OrcaFlex has some extra active settings that is not included in the toolkit, for instance, there might be some kind of structural damping that reduces the moment in OrcaFlex. To overcome this problem the irregular wave verification should be redone in OrcaFlex. Overall the verification results indicate that the sea loads has been implemented correctly.

11 Recommendations

To improve the pipe construction toolkit, the following actions are recommended:

- Solve the implicit equation 2.7.8 to obtain wave length for finite water depth.
- There are two irregular wave spectrums implemented in the toolkit, JONSWAP and Pierson-Moskowitz. More wave spectrums can easily be implemented if it is needed. Other common wave spectrums are for example Ochi-Hubble spectrum, Torsethaugen spectrum, Gaussian Swell spectrum.
- Implement the equal energy approach in the toolkit.
- Currently flexible Timoshenko beams are used to connect the cylindrical elements by the toolkit. OrcaFlex on the other hand uses translational and rotational springs and damper when modelling pipe structures. How the structure should be modelled need to be studied further.
- Currently a simple directional spectrum is used in the pipe construction toolkit. Since it is only valid for short crested waves, an additional directional spectrum valid for long crested waves should be added. Alternatively a single directional spectrum valid for both short crested and long crested waves should be added.
- Functionalities like wheeler stretching, directional spectrum, relative motion and the structural dynamics of the pipe are still left to be verified. Since the OrcaFlex moment in the irregular wave verification was consistently lower than the one in Adams the irregular wave verification should be remade. When recreating the OrcaFlex model more nodes should be used to check if the results converge. It is also important that all the active settings are investigated thoroughly in the OrcaFlex model, especially deactivate the seabed friction.
- When a directional spectrum is introduced the energy in the sea state changes. A user defined scaling factor should therefore be multiplied to the directional spectrum so that the user can control the energy in a sea state, see OrcaFlex Manual [10].
- Irregular waves are created by defining a lot of user parameters, it is therefore easy to get it wrong. Currently the user must run a simulation to see how the irregular waves turn out. This is unnecessary since the irregular waves are generated in the pipe construction macros. This makes it possible to see how the irregular waves turned out after the pipe is constructed. The toolkit could therefore be improved by plotting both the wave spectrum and the resulting irregular wave automatically after the pipe has been created.
- In reality the riser pipes are attached to a mobile structure at the top end. The motion of the top end is usually described with a response amplitude operator, RAO. To make a more realistic model an RAO should be implemented into the toolkit.
- Currently the pipe construction macros are adapted to build long straight pipes, the cylindrical elements could also be used to create other structures like flexible pipes.
- The toolkit needs extensive testing to debug and fix inflexibilities in the macros and in the dialog box.

- Insert help texts into the dialog box that explain the meaning of the parameters and give useful tips.

Bibliography

[1] O.M.Faltinsen *Sea loads on ships and offshore structures*. Cambridge: Cambridge University Press, 1990. pp 33-34

[2] Alexandra. H.Techet *Morrison's Equation* http://ocw.mit.edu/courses/mechanical-engineering/2-22-design-principles-for-ocean-vehicles-13-42-spring-2005/readings/r13_morrison.pdf. USA: Massachusetts Institute of Technology Dept. Mechanical Engineering Center for Ocean Engineering, 2004. pp 2

[3] Suphat Vongvisessomjai and Richard Silvester *Wave forces on submerged objects*. pp 2-3

[4] J.M.J.Journée and W.W Massie *Offshore hydromechanics*. Netherlands: Delft University of Technology, 2001. Chapter 5-1:17, 9-4, 12-5:3, 12-23:27, 12-5:3

[5] Robert A.Adams and Christopher Essex *Calculation - A complete course*.Seventh edition, Ontario: Person 2003. pp 685

[6] SNITEF marintek and the Norwegian Univeristy of Science and Technology *USFOS Hydrodynamics - Theory Description of use Verification*. www.usfos.no/manuals/usfos/verification/documents/Usfos_Hydrodynamics.pdf Norway. pp 54,66,67,56,64-65

[7] A.Boström *Rigid body dynamics*. Sweden: Chalmers University of Technology, 2009. Chapter 2, pp 27, https://www.student.chalmers.se/hp/hp/?hp_id=7741&hp_view=handout

[8] CODECOGS, 2013 *The JONSWAP spectra in the frequency domain*. http://www.codecogs.com/library/engineering/fluid_mechanics/waves/spectra/jonswap.php, 2013-12-17

[9] CODECOGS, 2013 *Defines the Pierson Moskowitz spectra in the wave-frequency domain*. http://www.codecogs.com/library/engineering/fluid_mechanics/waves/spectra/pierson_moskowitz.php, 2013-12-17

[10] Orcina Ltd., *OrcaFlex Manual Version 9.7a*, http://www.orcina.com/SoftwareProducts/OrcaFlex/Documentation/OrcaFlex.pdf,UK, 2013-03-21

Appendix

A Regular wave torque verification

To verify the torque calculation in a regular wave, a MATLAB model and an Adams model of a vertical pipe were created, see figure 9.3.1. The upper end of the pipe was fixed and the lower end was free. No current was applied to the model. The pipe was assumed to be rigid. The other parameters used in the model construction are listed below in table A.0.1. The simulations time was 20 s with the time step 0.1 s. The output of the simulations were the reaction forces in the fixed joint. The torques M_y from Adams and MATLAB are plotted in figure A.0.1 and the extreme values from both calculations were listed in table A.0.2. It can be seen that the maximums and minimums from MATLAB and Adams agree well. The same conclusions can be made by studying figure A.0.1.

Table A.0.1: Input for torque verification in a regular wave

Sea environment	
Density seawater [kg/m^3]	1024
Water depth [m]	100
Wave Parameters	
Wave Type	Regular
Wave Period [s]	20
Wave Amplitude [m]	7
Pipe parameters	
Upper end [m]	(0,0,10)
Lower end [m]	(0,0,-100)
Outer diameter [m]	0.05
Inner diameter [m]	0
Density pipe [kg/m^3]	7800
C_D	1
C_A	1

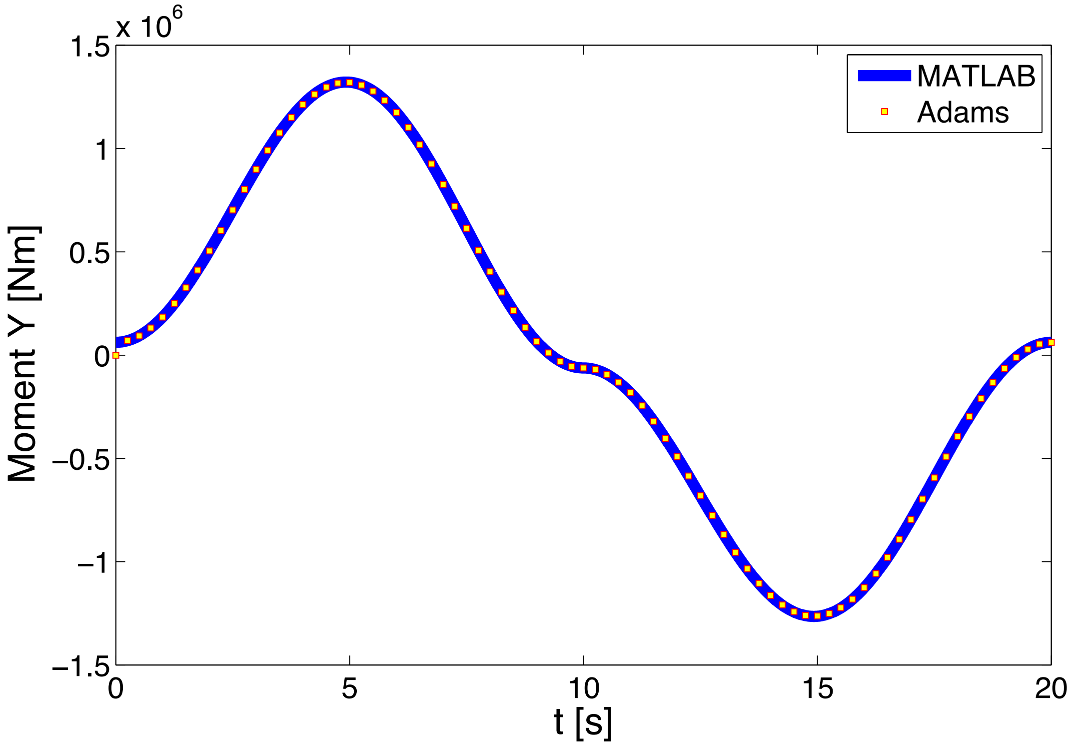

Figure A.0.1: *The torque M_y calculated in MATLAB and Adams*

Table A.0.2: The maximums and minimums for the calculated M_y in the joint from both MATLAB and Adams

M_y,[Nm]	MATLAB	Adams
maximum	1.3220e+06	1.3210e+06
minimum	-1.2649e+06	-1.2639e+06